

***Interlaboratory Round Robin
Axial Tensile Testing of
Tubular SiC/SiC Specimens***

**Nuclear Technology
Research and Development**

***Prepared for
U.S. Department of Energy
Nuclear Technology Research and
Development Advanced Fuels Campaign
G. Singh¹, S. Gonczy², E. Lara-Curzio¹
and Y. Katoh¹***

¹Oak Ridge National Laboratory

²Gateway Materials Technology, Inc.

August 25, 2017

M3FT-17OR020202103

Approved for public release. Distribution is unlimited



DISCLAIMER

This information was prepared as an account of work sponsored by an agency of the U.S. Government. Neither the U.S. Government nor any agency thereof, nor any of their employees, makes any warranty, expressed or implied, or assumes any legal liability or responsibility for the accuracy, completeness, or usefulness, of any information, apparatus, product, or process disclosed, or represents that its use would not infringe privately owned rights. References herein to any specific commercial product, process, or service by trade name, trade mark, manufacturer, or otherwise, does not necessarily constitute or imply its endorsement, recommendation, or favoring by the U.S. Government or any agency thereof. The views and opinions of authors expressed herein do not necessarily state or reflect those of the U.S. Government or any agency thereof.

SUMMARY

Extensive research and development work is being conducted at different governmental, university and industrial laboratories for developing accident tolerant fuel-cladding systems for light water reactors. Continuous SiC fiber-reinforced SiC matrix (SiC/SiC) composites is one of the candidate materials for replacing the traditional zirconium alloy cladding due to its high temperature stability, chemical inertness and stability under neutron irradiation. A comprehensive database on the statistics of the mechanical properties of SiC/SiC composite is much needed to estimate the failure probability in evolving thermo-mechanical conditions as well as rigorous analysis of the material's behavior under normal and off-normal reactor conditions. In addition to the properties database, test standards, which ensure the unbiased characterization of the material, are needed. The mechanical properties database, particularly for tubular SiC/SiC specimens, is limited and standardized test methods are still under development.

With the objective of expanding the database of mechanical properties of nuclear grade SiC/SiC and establishing the precision and bias statement for ASTM C1773 standard, an interlaboratory round-robin study was conducted on the tensile strength of SiC/SiC tubular specimens at room temperature. The mechanical properties statistics from the round robin study and the precision statistics and precision statement are presented herein. The data show reasonable consistency across the laboratories, indicating that the current C1773-13 ASTM standard is adequate for testing ceramic fiber reinforced ceramic matrix composite tubular specimens. Limited statistical variation in the mechanical properties show that the quality of the SiC/SiC material employed in these tests is adequate for meeting the nuclear applications. The ultimate tensile strength data seems to follow the Weibull distribution and the proportional limit strength data fit best with the lognormal distribution, for the tested SiC/SiC composite material.

CONTENTS

1.	INTRODUCTION	1
2.	TEST MATERIAL	3
2.1	SiC/SiC Composite - Fiber Matrix and Interphase	3
2.2	Reinforcement and Architecture	4
3.	METHOD	5
3.1	Pretest Procedure.....	5
3.1.1	Dimensional Measurement using Radiography	5
3.1.2	Alignment and Bending Minimization	6
3.2	Test Procedure.....	7
3.2.1	Grip Fixtures	7
3.2.2	Test Protocol and ASTM C1773-13 Standard	8
3.3	Post-Test Measurement and Analysis	9
3.3.1	Engineering Stress and Strain Calculation.....	9
3.3.2	Axial Tensile Strength and Strain Calculation.....	10
3.3.3	Fracture Strength and Strain Calculation	10
3.3.4	Young’s Modulus Calculation	10
3.3.5	Proportional Limit Stress and Strain Calculation	11
4.	RESULTS	11
4.1	Measured Properties and Distribution Fit	11
4.2	Precision and Bias Statements	17
5.	DISCUSSION.....	18
5.1	Effect of Dimension Measurement Technique on Statistics	18
5.2	Method for Measuring Young’s Modulus.....	20
5.3	Transition section failures vs Mid-Gage section failures.....	21
5.4	Failure mode.....	21
6.	SUMMARY.....	22
7.	REFERENCES	24

FIGURES

Figure 1: Cross-sectional planes of a SiC/SiC tubular specimen as observed by optical microscopy (top, lower left) and scanning electron microscopy (lower right).	4
Figure 2: An axial tensile test specimen with steel end plugs.	5
Figure 3: Radiography image of a tensile test specimen (a); locations for dimension measurement (outer and inner diameters) along the gage length (b) and angular locations for dimension measurement (c).....	6

Figure 4: Sketch of an alignment specimen showing strain gage locations.	6
Figure 5: An alignment specimen used for aligning the top and bottom fixtures and minimize the bending in the test specimen.....	7
Figure 6: Passive fixture for gripping the specimen during the axial tensile tests.	8
Figure 7: Annealed copper collets with tapered inner surface.....	8
Figure 8: Swivel joints employed to minimize the bending which occurs due to various sources including the irregular geometry of the specimen.....	8
Figure 9: A specimen in the ORNL test rig.....	9
Figure 10: Determination of ultimate tensile strength, Young’s modulus and proportional limit stress from the stress-strain curve. Proportional limit stress is based on 0.01% strain offset.	11
Figure 11: Ultimate tensile strength (UTS) and proportional limit stress (PLS) for each laboratory obtained from interlaboratory round robin testing (Error bar: ± 1 standard deviation about the mean).	13
Figure 12: Strain at failure and strain at proportional limit stress (PLS) for each laboratory obtained from interlaboratory round robin testing (Error bar: ± 1 standard deviation about the mean).	13
Figure 13: Fit of ultimate tensile strength data from interlaboratory round robin testing to different probability distribution functions, with 95% confidence bound lines in red.....	14
Figure 14: Fit of proportional limit stress data from interlaboratory round robin testing to different probability distribution functions, with 95% confidence bound lines in red.	15
Figure 15: Weibull distribution based 95% confidence bounds for ultimate tensile strength.	16
Figure 16: Lognormal distribution based 95% confidence bounds for proportional limit stress.	17
Figure 17: Measurements on a specimen wall; the surface roughness of the composite specimen leads to inaccurate measurement of the wall thickness by caliper, compared to radiography.....	19
Figure 18: Proposed method to determine the Young’s modulus and proportional limit stress.....	20
Figure 19: Specimens with failure in transition section (leftmost specimen) and mid-gage section.	21
Figure 20: A typical tensile stress-strain curve obtained from the round robin tests.	22
Figure 21: SEM image of the fractured cross-section surface of a tested SiC/SiC tubular specimen.	22
Figure 21: Stress-strain curve for specimen-9.	4
Figure 22: Stress-strain curve for specimen-10.	4
Figure 23: Stress-strain curve for specimen-11.	5
Figure 24: Stress-strain curve for specimen-12.	5
Figure 25: Stress-strain curve for specimen-13.	6

TABLES

Table 1: Typical properties of SiC/SiC composite tubular specimens at room temperature. Source [12, 15-17, 29-32].....	4
Table 2: Results from the interlaboratory round robin axial tensile testing of SiC/SiC tubular specimens.	14
Table 3: Goodness of fit statistics for each distribution fit to the strength data. Lower statistics indicate a better fit.	16
Table 4: Precision statistics calculated from the interlaboratory round robin data.....	18
Table 5: Comparison of dimensions of SiC/SiC tubular specimens (7 specimen) measured using radiography and vernier caliper.....	19
Table 6: Comparison of properties evaluated using radiography and caliper based dimensions for laboratory Lab5.	19
Table 7: Comparison of the material properties obtained from the specimens that failed in the mid-gage section and transition section.	22

ACRONYMS

AE	Acoustic emission
AFC	Advanced Fuels Campaign
ASTM	American Society for Testing and Materials
ATF	Accident-tolerant fuel
CFCC	Continuous fiber-reinforced ceramic matrix composite
CMC	Ceramic matrix composite
DOE-NE	US Department of Energy Office of Nuclear Energy
ID	Inner diameter
ILS	Interlaboratory study
LWR	Light water reactor
OD	Outer diameter
ORNL	Oak Ridge National Laboratory
PLS	Proportional limit stress
PWR	Pressurized water reactor
RT	Room temperature
SiC	Silicon Carbide
SiC/SiC	Silicon carbide fiber-reinforced silicon carbide matrix composite
UTS	Ultimate tensile strength

INTERLABORATORY ROUND ROBIN TESTING OF TUBULAR SiC/SiC SPECIMENS

1. INTRODUCTION

Background and Objectives

Silicon carbide (SiC) fiber-reinforced SiC matrix composites (SiC/SiC composites) offer a set of properties that make these materials highly suitable for many high temperature applications. Like monolithic SiC ceramics SiC/SiC composites maintain their mechanical properties and chemical inertness even at temperatures beyond the upper limit for typical metallic superalloys. These composite materials have high specific strength and reasonable damage tolerance. Some of the applications for which SiC/SiC composites are being considered include heat exchangers, reformers, reactors and filters in chemical industry, preheaters, recuperators and radiation tubes in heat transfer systems, space vehicles, components of furnaces, gas turbine engines and nuclear reactors.

The Fukushima Daiichi nuclear power plant accident led to world-wide spread safety concerns over existing nuclear reactors around the globe. In efforts to enhance the safety of nuclear power plants extensive research and development work on improving the accident tolerance of fuel-cladding systems is being conducted [1, 2]. Because of the stability of SiC/SiC composites under neutron irradiation conditions, low activation and other properties as mentioned above, SiC/SiC is a promising candidate material for the accident tolerant fuel cladding systems in light water reactors (LWR) [3, 4]. It should be noted here that the stability under irradiation is a unique property of SiC/SiC composites, which is not exhibited by other composites including those reinforced by carbon fibers. Besides application in LWRs, SiC/SiC composites have potential structural and insulation applications in other nuclear energy systems, such as Very High Temperature Reactor (VHTR) [5, 6], Gas-Cooled Fast Reactor (GFR) [7], Molten Salt Reactor (MSR), sodium fast reactor (SFR), and fusion reactors [8, 9]. Although SiC/SiC composites are manufactured in the forms of chopped fiber composites, particulate-reinforced composites and continuous fiber composites, only continuous fiber SiC/SiC composites are suitable for fuel cladding fabrication.

The deployment and commercialization of components for nuclear technologies manufactured using SiC/SiC composite, require several considerations including critical feasibility [10]. A “qualified” database of properties of SiC/SiC composite will be needed for performing rigorous experimental and numerical studies to determine the viability of the material for specific applications. In general, a “qualified” database is one which is generated using procedures which comply with standards associated with the design code of the component of interest. In the absence of a qualified database, the studies for assessment of the material either cannot be carried out or the results of the studies cannot be interpreted and applied with confidence, leading to designs with high safety margins. Besides, the designer cannot use a material (without a database) directly in new designs but has to 1) provide evidence that the material complies with the code requirement and 2) obtain permission to use that material in design [11]. Thus, lack of a comprehensive property database can significantly hamper the development of the technology and can negatively affect the material development.

Nuclear grade SiC/SiC composite consists of near-stoichiometric and crystalline beta-phase SiC for both fibers and matrix, and less-radiation-stable interphase which is the material between the fibers and

matrix. The current database of mechanical properties for nuclear grade SiC/SiC composite is limited. Although various properties of nuclear grade SiC/SiC composites have been measured, tubular test specimens were not used in those studies [12]. Most of the studies utilized rectangular bars and disc specimens for thermo-mechanical and physical property evaluations. The ASTM standard test methods for axial tensile test (ASTM C1773-13) and hoop tensile test (ASTM C1819-15) of continuous-fiber reinforced ceramic composite tubes have been developed and become available only recently. However, these two ASTM standards lack the precision and bias statements which convey important information to the users of the ASTM standard about the quality of their test results. In other words, these standards need round-robin studies to develop precision and bias statements.

Several studies [13-17] have been conducted in the past to evaluate the properties of SiC/SiC composites. Nozawa et al. [13] conducted tensile and compressive tests on flat specimens of three types of composites: plain-weave CVI, plain-weave NITE and unidirectional NITE SiC/SiC composites. It was found that for tensile loading, Young's modulus, proportional limit stress (PLS) and fracture strength decreased with increase in the angle between the fiber orientation and the load direction, while the Poisson's ratio increased. The study also demonstrated that the Tsai-Wu [14] criterion can model the effect of anisotropy on the in-plane tensile and compressive stresses. In another study, Rohmer et al. [15] conducted axial and hoop tensile tests on CVI SiC/SiC tubular specimens which had fiber braids oriented at $\pm 30^\circ$ with the tube axis. The axial tensile strength (463 MPa) and axial PLS (82 MPa) were found to be much greater than the hoop tensile strength (63 MPa) and hoop PLS (36 MPa). The axial and hoop Young's moduli were reported to be 232 GPa and 158 GPa, respectively. Both the studies by Nozawa et al. [13] and Rohmer et al. [15] demonstrated the strong influence of fiber orientation on the mechanical properties of SiC/SiC composite. Deck et al. [16] conducted hoop tensile tests and uniaxial tensile tests on CVI SiC/SiC composites. Hoop test were conducted through C-ring tests as well as expanding plug tests. The study involved hoop biased (fiber reinforcement greater in hoop direction by 1.5:1 ratio), axial biased (1.3:1) and unbiased tubular specimens. The reported results show a significant effect of biasing on the Young's modulus and strength properties of the material. Bernachy-Barbe et al. [17] conducted several mechanical tests and reported modulus, tensile, compressive and shear strength data for CVI SiC/SiC specimens. Despite these studies, the database for this material is still far from being comprehensive.

The current work described in this paper aims to fill these gaps in the development process of SiC nuclear fuel cladding technology. An interlaboratory round robin study on the tensile properties of SiC/SiC tubular specimens was conducted with participating laboratories from government institutions, academia and industry. This interlaboratory study served multiple objectives: 1) Expand the limited database of mechanical properties of SiC/SiC composite tubular structures and 2) Develop precision statement for the ASTM C1773 Standard Test Method (Monotonic Axial Tensile Behavior of Continuous Fiber-Reinforced Advanced Ceramic Tubular Test Specimens at Ambient Temperature).

Test Procedure

These objectives were accomplished through an interlaboratory round robin study which was conducted according to the ASTM E691-09 standard: Standard Practice for Conducting an Interlaboratory Study to Determine the Precision of a Test Method. Primary mechanical properties of interest include axial elastic modulus, axial proportional limit stress and the corresponding strain, ultimate tensile strength and the corresponding strain. As a first step ORNL performed the lead test to identify any potential issues with the testing of the SiC/SiC tubular specimens and the test protocol was prepared addressing those issues.

The findings from the lead test were also discussed with the specimen provider General Atomics, and the specimen design was modified accordingly. The objective of the test protocol was to help the interlaboratory participants to rigorously implement the ASTM C1773-13 requirements and fulfill the specific requirements pertaining to the testing of the SiC/SiC tubular specimens employed in this study. After the completion of the ORNL lead test, the specimens, fixtures and other parts for testing were distributed to the interlaboratory study participants. The participating laboratories independently tested the specimens according to the test protocol and reported the test results in a set duration of time. Reports by the various laboratories were collected by ORNL which performed the analysis of the results.

2. TEST MATERIAL

2.1 SiC/SiC Composite - Fiber Matrix and Interphase

In this study 47 nuclear grade SiC/SiC composite specimens were tested by seven laboratories for tensile properties at room temperature. Four specimens could not be tested successfully, therefore, the data from 43 specimens were used for calculating the statistics. The tubular specimens were specifically designed for the interlaboratory round robin testing and contained Hi-Nicalon™ Type S fibers. These fibers are near stoichiometric (manufacturer-claimed C/Si atomic ratio of ~1.05), stable under neutron irradiation, show limited irradiation creep [18] and can maintain thermal creep strength up to 1400°C [19]. The fibers have a typical chemical composition of Si:C:O as 69:31:0.2 wt% and the tensile strength and tensile modulus are 2.6 GPa and 420 GPa, respectively [20, 21]. The typical filament diameter and density are 11 μ and 3.10 g/cc. These fibers are commercially produced by NGS Advanced Fibers Co. (Toyama, Japan). Extensive research efforts on the development of these fibers are presented in reference [22].

A 150nm thick monolayer of pyrocarbon (PyC) forms the interphase coating between the fiber and matrix in the SiC/SiC composite used for this work. The interphase coating plays an important role in imparting mechanical properties to SiC/SiC composites; interphase material is weaker and more compliant than both fiber and matrix, and it deflects cracks propagating through the matrix, thus preventing fiber cracking and breakage. The interphase coating imparts pseudo ductility to the composite material by allowing the fibers to debond and slide and to bridge matrix cracks. For nuclear applications only PyC or PyC/SiC are suitable choices [23].

The tubular specimens used in this study have high-purity SiC matrix. Similarly, to the fibers, only near stoichiometric matrices with high crystallinity and a minimum of secondary phases are stable in irradiation environments. Of the several techniques available to densify the matrix, CVI has been found to produce a SiC matrix of the required quality [24]. Besides, the Nano-Infiltration and Transient Eutectic-Phase (NITE) process has also been found to produce SiC/SiC composites that are stable under irradiation [25-27]. The CVI process was used in this work to prepare the SiC/SiC specimens.

In addition to the material constituents, the fiber architecture and the associated properties were selected such that the specimens represented a typical accident tolerant fuel cladding. The strength degradation of the SiC/SiC composite material by irradiation occurs only at high doses [28]. The swelling and change in the thermal conductivity of the SiC/SiC composite saturates at about 1 dpa [28]. The typical properties of SiC/SiC composite tubular specimens are listed in Table 1. Figure 1 shows the cross-section micrographs of the SiC/SiC tubular specimen at two length scales, illustrating the internal porosity that is characteristics of chemical vapor infiltration and the undulation of the outer and inner surfaces of the structure.

Table 1: Typical properties of SiC/SiC composite tubular specimens at room temperature. Source [12, 15-17, 29-32]

Property	Value
Density	2.3 – 2.8 g/cm ³
Porosity	10 – 20%
Fiber volume fraction	30 – 40%
Young's modulus	170 – 250 GPa (tensile) 250 GPa (compressive)
Shear modulus	80 – 120 GPa reported for flat specimens
Poisson's ratio	~0.13 for 0°/90°, ~0.25 for ±45° (in-plane) for flat specimens
Proportional limit stress	80 – 110 MPa (axial) 100 – 160 MPa (hoop)
Ultimate tensile strength	230 – 270 MPa (axial) 200 – 340 MPa (hoop)

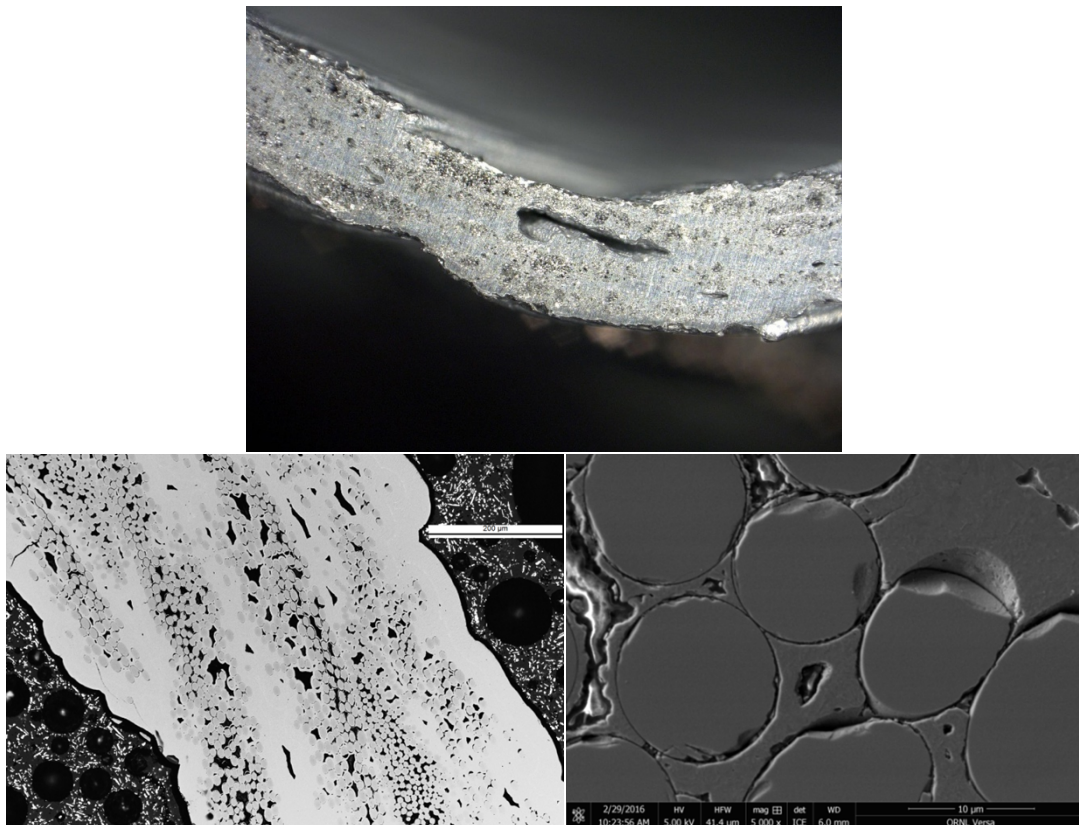


Figure 1: Cross-sectional planes of a SiC/SiC tubular specimen as observed by optical microscopy (top, lower left) and scanning electron microscopy (lower right).

2.2 Reinforcement and Architecture

Silicon carbide fibers are typically produced as single multifilament tows. These tows are then woven or knitted to form a variety of fabric types, including preforms. Preforms are a type of fabric form suited for a particular application in terms of shape, mechanical and structural requirements. Fiber preforms for the test material were fabricated using triaxial braiding. This weaving style allows the fabric to conform to complex shapes and retains balance on both side of the fabric. The fiber tow bundles were

stacked in $\sim\pm 55^\circ$ orientation with fiber bundles at 0° direction for axial reinforcement. The fiber volume fraction was about 51%.

The density and porosity of the material was $2.6 - 2.8 \text{ g/cm}^3$ and $\sim 13.5\%$, respectively. An axial tensile test specimen is shown in Figure 2. The specimens are 150 mm in length with 8° tapered shoulders. The nominal wall thickness, outer diameter and gage section length are 0.8 mm, 9.5 mm and 70 mm respectively. Figure 2 shows the steel end plugs bonded into the shoulder sections that prevent crushing in the grip fixtures.



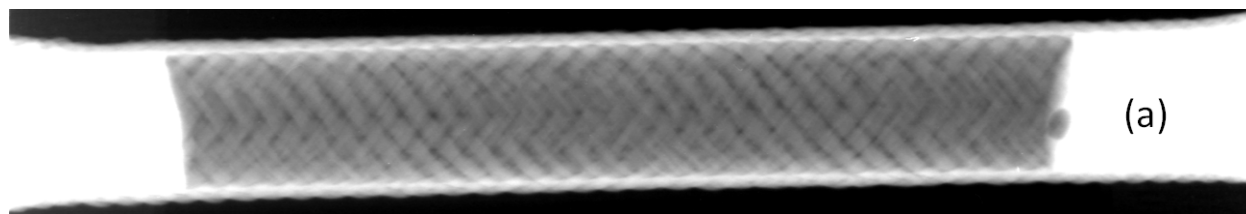
Figure 2: An axial tensile test specimen with steel end plugs.

3. METHOD

3.1 Pretest Procedure

3.1.1 Dimensional Measurement using Radiography

The dimensions of all the specimens (outer and inner diameters) were measured at ORNL using radiography. The accuracy of the measurements was $\pm 0.02 \text{ mm}$. The radiography images for each specimen were taken at three angles 0° , 60° and 120° as shown in Figure 3. For each image the dimensions were measured at three different locations along the gage length. The outer and inner diameters were calculated as the average of these 9 measurements. The wall thickness of the specimen was calculated from the difference of the average outer and inner diameters. The average outer diameter, inner diameter and wall thickness for all the specimens were measured to be 9.53 mm, 7.97 mm and 0.78 mm respectively. The standard deviation (measured from 43 specimens) in the mean OD, ID and wall thickness of all the specimen were 0.062 mm, 0.060 mm and 0.027 mm, respectively.



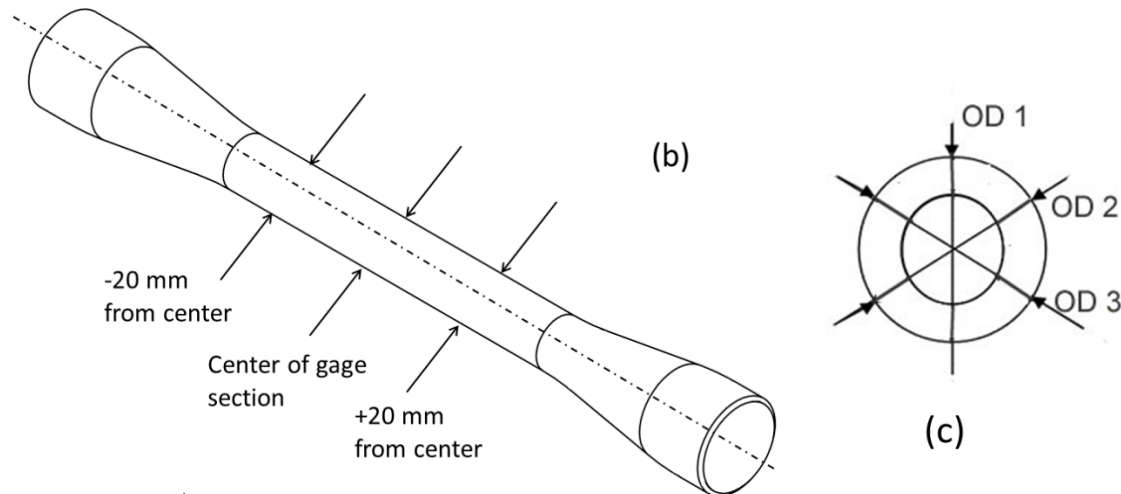


Figure 3: Radiography image of a tensile test specimen (a); locations for dimension measurement (outer and inner diameters) along the gage length (b) and angular locations for dimension measurement (c).

3.1.2 Alignment and Bending Minimization

There have been no studies conducted for studying the effect of bending in the specimen on the tensile strength distribution of CFCCs. However, for monolith advanced ceramics such studies have been conducted and it is concluded that the bending in the specimen should not exceed 5% to keep the effects of bending on the strength distribution parameters negligible. Figures 4 and 5 show the alignment specimen used for performing the load train alignment. These alignment specimens employed strain gages with linear pattern (gage designation: C2A-06-125LW-350); the gages were obtained from Vishay Precision Group Inc. Because the SiC/SiC composite and steel have nearly equal Young's modulus (≈ 205 GPa), steel was selected as the material for the alignment specimens.

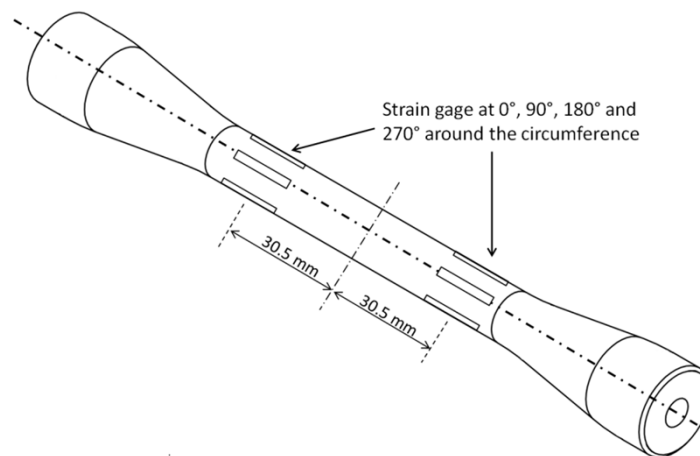


Figure 4: Sketch of an alignment specimen showing strain gage locations.



Figure 5: An alignment specimen used for aligning the top and bottom fixtures and minimize the bending in the test specimen.

The bending in the specimen is calculated as:

$$\text{Bending (\%)} = \frac{\varepsilon_b}{\varepsilon_0} \times 100 \quad (1)$$

$$\varepsilon_b = \left[\left(\frac{\varepsilon_1 - \varepsilon_3}{2} \right)^2 + \left(\frac{\varepsilon_2 - \varepsilon_4}{2} \right)^2 \right]^{1/2} \quad (2)$$

$$\varepsilon_0 = \frac{\varepsilon_1 + \varepsilon_2 + \varepsilon_3 + \varepsilon_4}{4} \quad (3)$$

where ε_1 , ε_2 , ε_3 and ε_4 are the strains measured by the strain gages located at 0° , 90° , 180° and 270° respectively.

3.2 Test Procedure

3.2.1 Grip Fixtures

There are two types of grip fixtures that are commonly used for testing CMC specimens with tubular geometry: active and passive. The passive grip fixtures do not require a direct application of gripping force; rather, the axial force applied by the test machine is employed to generate compressive force on the fixture either through adhesive bond or by mechanical features in the grips. For this work passive grip fixtures were used. Figure 6 shows the fixture employed for gripping the tubular specimens. The test specimen is directly in contact with the copper collets (see Figure 7) which served the dual function of holding the specimen inside the fixture and also minimizing the bending in the specimen by deforming and realigning itself in response to the bending moment. The specimens had adhesively bonded steel end plugs to prevent crushing in the grip sections of the test specimen, as shown in Figure 2.

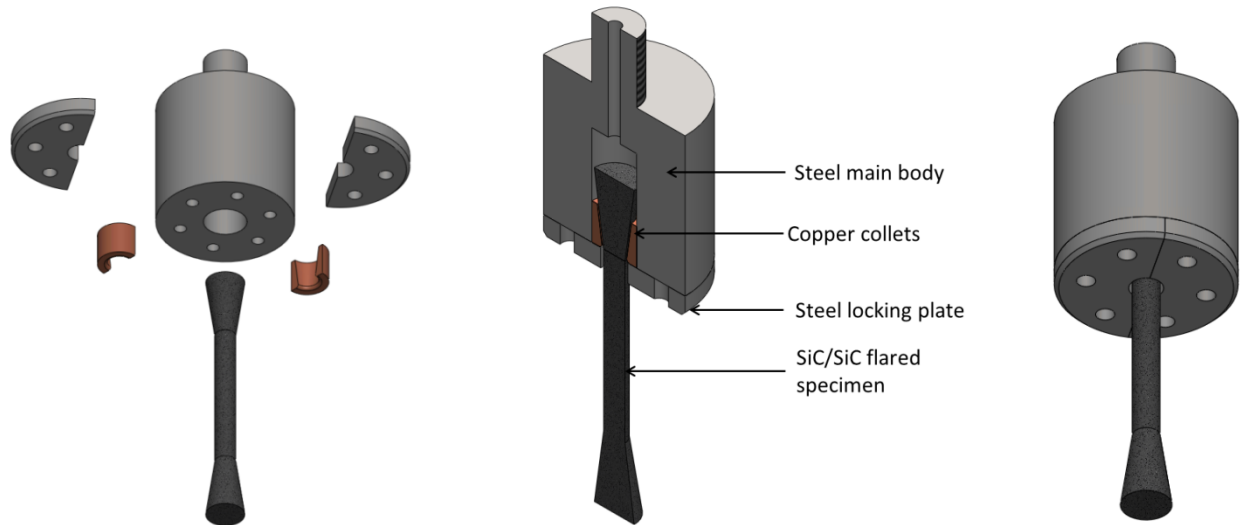


Figure 6: Passive fixture for gripping the specimen during the axial tensile tests.

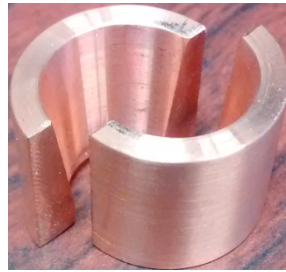


Figure 7: Annealed copper collets with tapered inner surface.

3.2.2 Test Protocol and ASTM C1773-13 Standard

The standard test method ASTM C1773-13 (Standard Test Method for Monotonic Axial Tensile Behavior of Continuous Fiber-Reinforced Advanced Ceramic Tubular Test Specimens at Ambient Temperature) was used to conduct the axial tensile test on SiC/SiC tubular specimens. Prior to the test the top and bottom fixtures were aligned to reduce the unwanted bending. To further reduce bending, swivel joints were also used to connect both ends of the test specimen to the load train (see Figure 8).



Figure 8: Swivel joints employed to minimize the bending which occurs due to various sources including the irregular geometry of the specimen.

Unlike their monolith counterparts, which undergo catastrophic fracture, continuous fiber-reinforced ceramic matrix composite (CMC) accumulate damage during the loading process. Due to the

gradual damage process, CMCs exhibit a non-linear stress-strain behavior after the elastic limit. (See Figure 10) So, displacement controlled tests were employed to prevent “run away” condition – a rapid uncontrolled deformation and fracture. The test machine was set up for an initial cross-head position, zero load, and displacement mode and a displacement rate of 0.76 mm/min. The specimens were preloaded to 30–40N. The strain was measured with extensometer. Figure 9 shows a specimen while being tested in the Oak Ridge National Laboratory test rig. Acoustic sensors were used to understand the progressive damage in the SiC/SiC specimen.

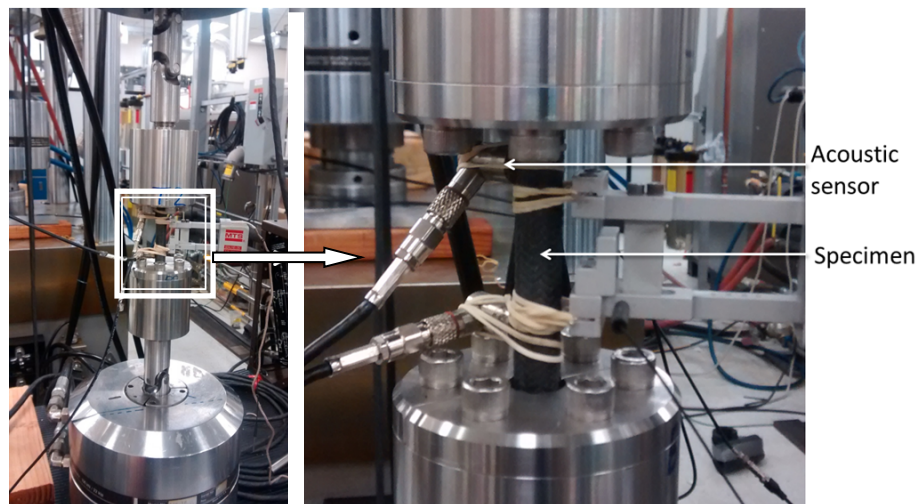


Figure 9: A specimen in the ORNL test rig.

3.3 Post-Test Measurement and Analysis

After the completion of the test, the gage section outer diameter (OD), inner diameter (ID) and fracture location are measured. The fracture locations relative to the midpoint of the gage section are measured. Using visual examination, optical microscopy and electron microscopy the fracture surfaces are analyzed to determine the mode and type of fracture.

3.3.1 Engineering Stress and Strain Calculation

The engineering stress is calculated as:

$$\sigma = \frac{P}{A} \quad (4)$$

where:

σ : the engineering stress in units of MPa,

P : the applied uniaxial tensile load in units of N, and

A : the average original cross-section area of the tube specimen in units of mm²

The cross-sectional area A is calculated as:

$$A = \frac{\pi(d_o^2 - d_i^2)}{4} \quad (5)$$

where

d_o : the average outer diameter of the gage section in units of mm

d_i : the average inner diameter of the gage section in units of mm

The engineering strain, measured by the extensometer, is calculated as:

$$\varepsilon_{yy} = \frac{l - l_0}{l_0} \quad (6)$$

where

ε_{yy} : the axial engineering strain (dimensionless)

l : the extensometer gage length at any time in units of mm

l_0 : the original extensometer gage length in units of mm

3.3.2 Axial Tensile Strength and Strain Calculation

The axial tensile strength is calculated as:

$$S_u = \frac{P_{\max}}{A} \quad (7)$$

where:

S_u : the tensile strength in units of MPa,

P_{\max} : the maximum force before failure in units of N, and

A : the average original cross-section area of the tube specimen in units of mm²

The axial strain at tensile strength is measured as the axial engineering strain (equation 3) corresponding to the tensile strength measured during the test.

3.3.3 Fracture Strength and Strain Calculation

The axial fracture strength is calculated as:

$$S_f = \frac{P_{\text{fracture}}}{A} \quad (8)$$

where:

S_f : the fracture strength in units of MPa,

P_{fracture} : the force corresponding to the fracture in units of N, and

A : the average original cross-section area of the tube specimen in units of mm²

The axial strain at fracture strength is measured as the axial engineering strain (equation 3) corresponding to the fracture strength measured during the test.

3.3.4 Young's Modulus Calculation

The modulus of elasticity is determined from the slope of the line fitted to the linear portion of the stress-strain curve using linear regression (see Figure 10).

3.3.5 Proportional Limit Stress and Strain Calculation

The proportional limit stress (PLS), σ_o , can be defined in several ways: offset method, extension under force method and deviation from linearity method. The offset method is used for determining the PLS for the current work. For CFCC the failure strain is relatively lower than other materials for which a typical 0.5% offset strain is used to determine the PLS. So an alternate offset strain of 0.01% is employed. Figure 10 shows the procedure for determining the PLS using the offset strain of 0.01%. A line is generated with its origin at zero stress and 0.01% strain, and running parallel to the linear portion of the stress-strain curve which was used to calculate the elastic modulus. The stress corresponding to the point where this line intersects the stress-strain curve is defined as the PLS. The strain at PLS is measured as the axial engineering strain (equation 3) corresponding to the PLS.

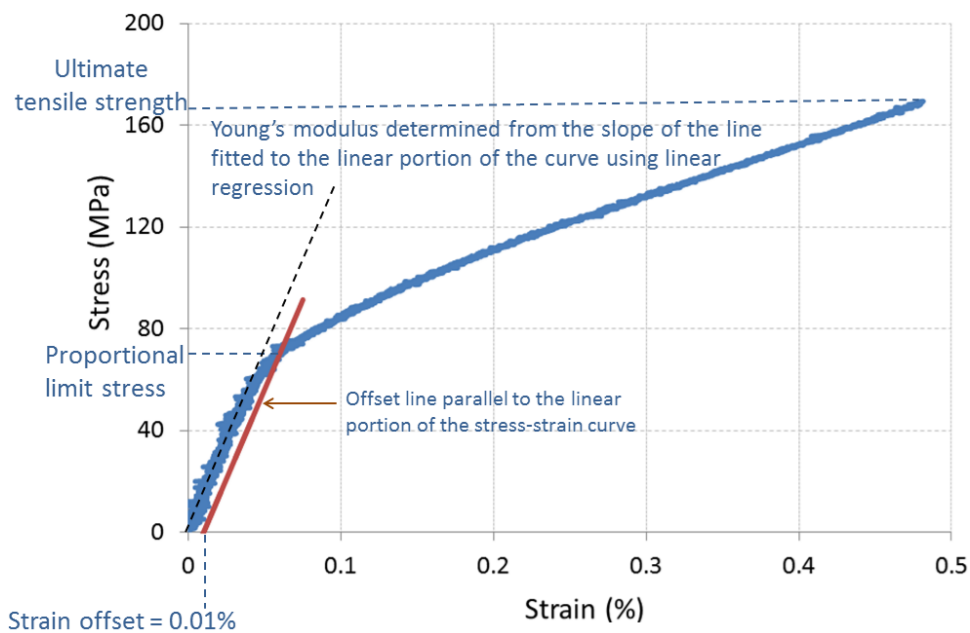


Figure 10: Determination of ultimate tensile strength, Young's modulus and proportional limit stress from the stress-strain curve. Proportional limit stress is based on 0.01% strain offset.

4. RESULTS

4.1 Measured Properties and Distribution Fit

In this round robin testing program the participating organizations are not identified, but they are distinguished by assigning them a numerical ID. Table 2 below lists the data for ultimate tensile strength (UTS), proportional limit stress (PLS), Young's modulus, strain at failure and strain at proportional limit stress obtained by the seven laboratories. For comparing across laboratories, strength and strain data are shown in figures 11 and 12 respectively. Figures 13 and 14 show the fit of several probability distributions to the global UTS and PLS data sets respectively.

The UTS was found to be consistent across the specimens with the small all-laboratories coefficient of variance (COV) of 12.5%. As can be noted from Figure 11, the individual laboratory means ranged from 220 to 257 MPa; the small range indicates consistency across the laboratories. However, the COVs for individual laboratories ranged from 5.5% to 19.8% indicating significant variation in the with-in lab spread

of the UTS data across the seven laboratories. Thus, the test operator and the test equipment can significantly contribute to the variation in the UTS property of SiC/SiC material. From the goodness of fit test (see Figure 13 and Table 3) it can be inferred that a 2-parameter Weibull distribution describes the UTS data best. The shape and scale parameters for the Weibull distribution fit were calculated to be 10.1 and 249.1.

The all laboratory mean for PLS was found to be 92.6 MPa with COV of 9.7% indicating consistency in the PLS property across the specimens. The laboratory means ranged from 79.8 MPa to 97.6 MPa as shown in Figure 11. The with-in lab COVs for PLS ranged from 6.3% to 13.4%. Except for Lab3 COVs were under 10% indicating a high consistency in the PLS property within and across the laboratories. As can be noted from Figure 14 and Table 3, the goodness of fit test showed that the Lognormal distribution fits best the PLS data with the log mean and log standard deviation as 4.52 and 0.096.

The all laboratory mean for Young's modulus was found to be 202.7 GPa with COV of 19.9%. The laboratory mean varied for 146.5 MPa to 240.4 MPa and the COV ranged from 6.0% to 22.6%. A large variation in the mean may be due to the due to inconsistency in the method of calculating modulus from the stress-strain data. A relevant discussion is presented in section 5.2.

Table 2: Results from the interlaboratory round robin axial tensile testing of SiC/SiC tubular specimens.

Test Count	Ultimate Tensile Strength (MPa)		Proportional Limit Stress (MPa)		Young's Modulus (GPa)		Strain at Failure (%)		Strain at Proportional Limit Stress (%)		
	Mean	COV(%)	Mean	COV(%)	Mean	COV(%)	Mean	COV(%)	Mean	COV(%)	
Lab1	5	220.0	12.6	95.9	9.5	210.8	16.2	0.46	17.9	0.056	6.6
Lab2	7	245.6	6.0	85.6	9.1	191.4	6.0	0.57	8.5	0.056	8.8
Lab3	6	256.7	6.5	79.8	13.4	146.5	9.2	0.63	7.5	0.059	10.7
Lab4	6	220.8	19.8	99.8	9.0	232.4	13.5	0.46	28.2	0.063	15.4
Lab5	7	233.2	19.4	91.2	9.8	202.4	9.7	0.52	26.7	0.055	8.9
Lab6	5	242.6	5.5	93.8	6.6	189.7	22.6	0.53	8.9	0.055	11.3
Lab7	7	236.2	8.0	97.6	6.3	240.4	17.8	0.53	9.9	0.052	13.0
All Labs	43	236.8	12.5	92.6	9.7	202.7	19.9	0.53	18.5	0.057	12.0
Labs Statistics*		236.4	5.6	92.0	7.7	201.9	15.4	0.52	8.5	0.057	6.1

*For Labs Statistics row, Mean represents the mean of the laboratory means, COV represents the coefficient of variance of the laboratory means.

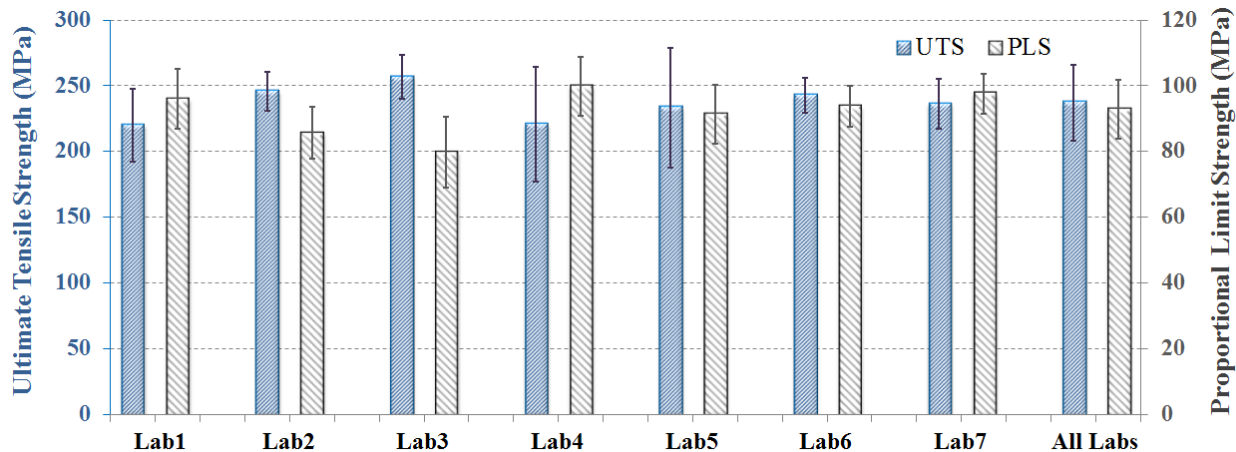


Figure 11: Ultimate tensile strength (UTS) and proportional limit stress (PLS) for each laboratory obtained from interlaboratory round robin testing (Error bar: ± 1 standard deviation about the mean).

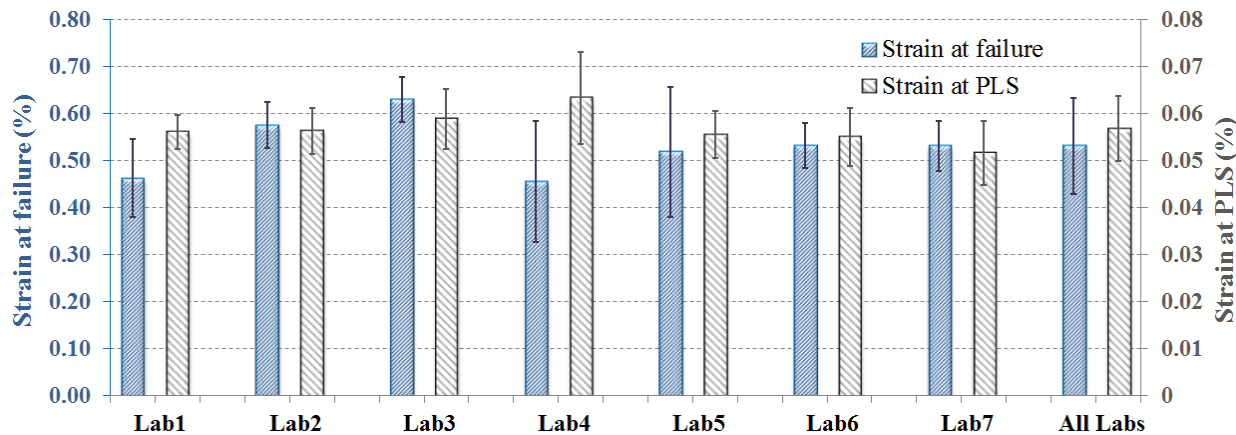


Figure 12: Strain at failure and strain at proportional limit stress (PLS) for each laboratory obtained from interlaboratory round robin testing (Error bar: ± 1 standard deviation about the mean).

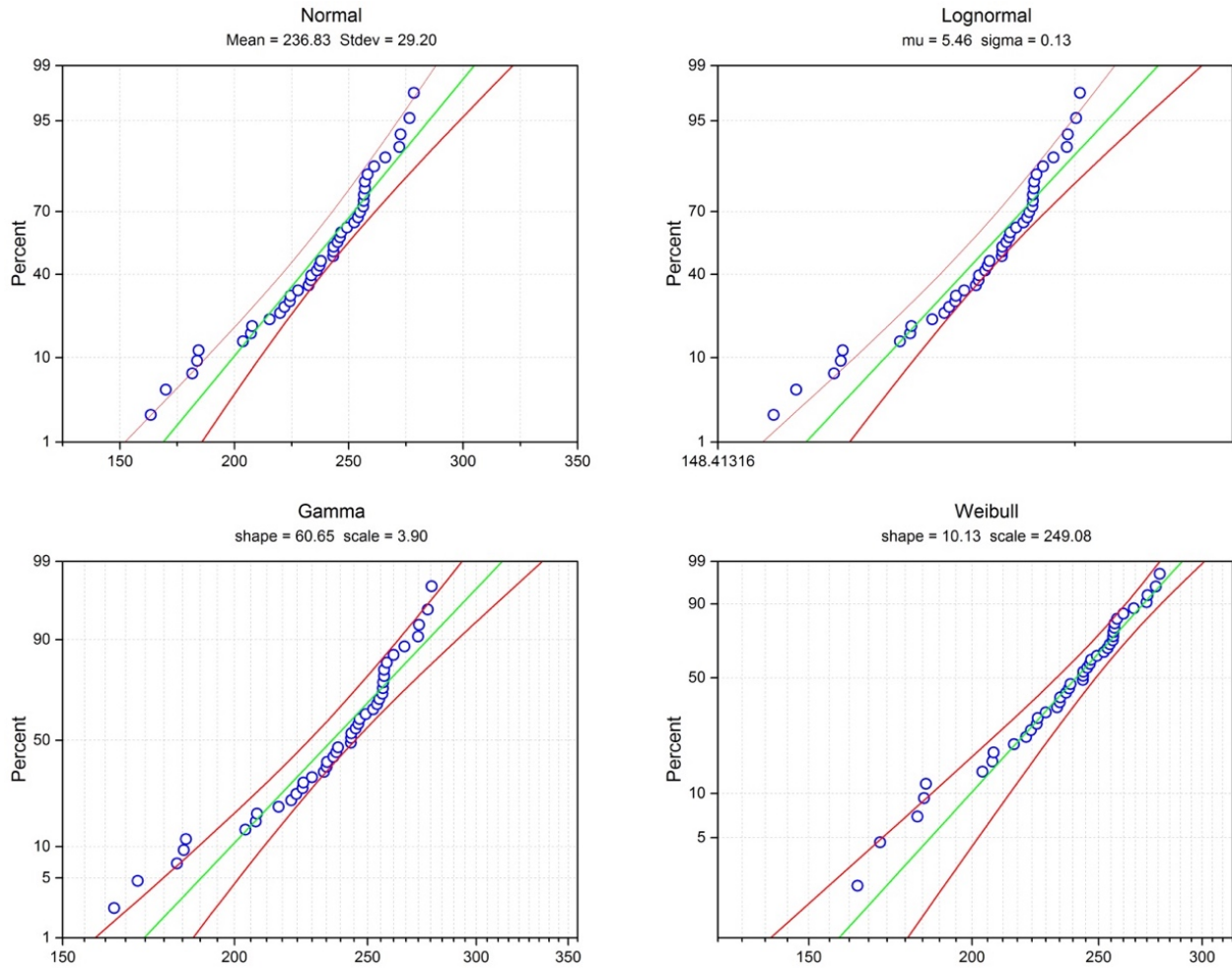


Figure 13: Fit of ultimate tensile strength data from interlaboratory round robin testing to different probability distribution functions, with 95% confidence bound lines in red.

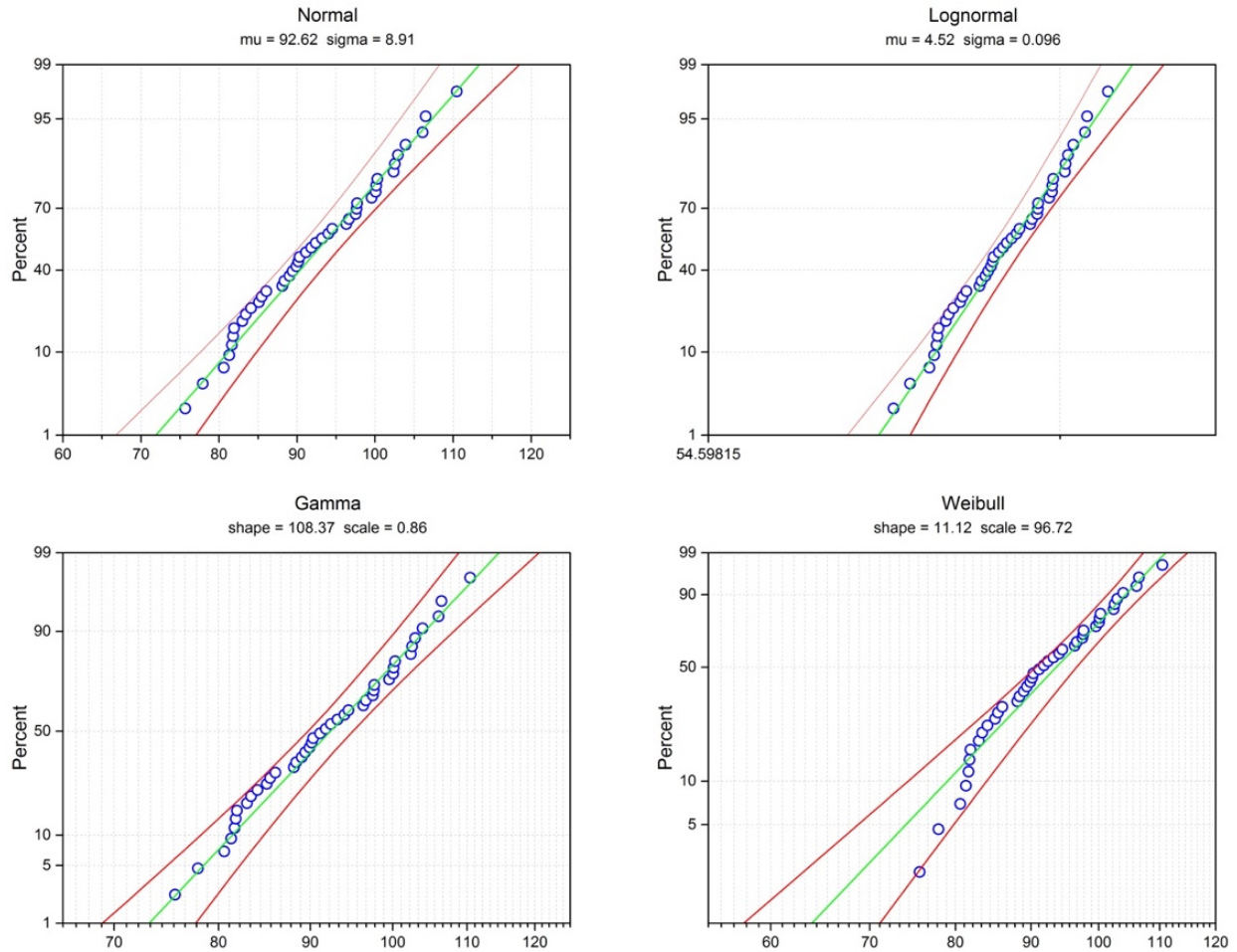


Figure 14: Fit of proportional limit stress data from interlaboratory round robin testing to different probability distribution functions, with 95% confidence bound lines in red.

**Table 3: Goodness of fit statistics for each distribution fit to the strength data.
Lower statistics indicate a better fit.**

	Distribution	Statistics
Ultimate tensile strength	Normal	0.097
	Lognormal	0.119
	Weibull	0.074
	Gamma	0.110
Proportional limit stress	Normal	0.072
	Lognormal	0.065
	Weibull	0.092
	Gamma	0.068

Figures 15 and 16 show the 95% confidence bounds for the Weibull and Lognormal distributions fit to the UTS and PLS data, respectively. For individual laboratories, the confidence bounds are significantly larger than the confidence bound for all laboratories data, due to the small number of specimens per lab (5-7). However, fair overlapping of confidence bounds indicates similar data statistics for the laboratories. For PLS the confidence bounds overlap well indicating very similar statistics for PLS across the laboratories. The confidence bounds for all laboratories data are also shown in the figures.

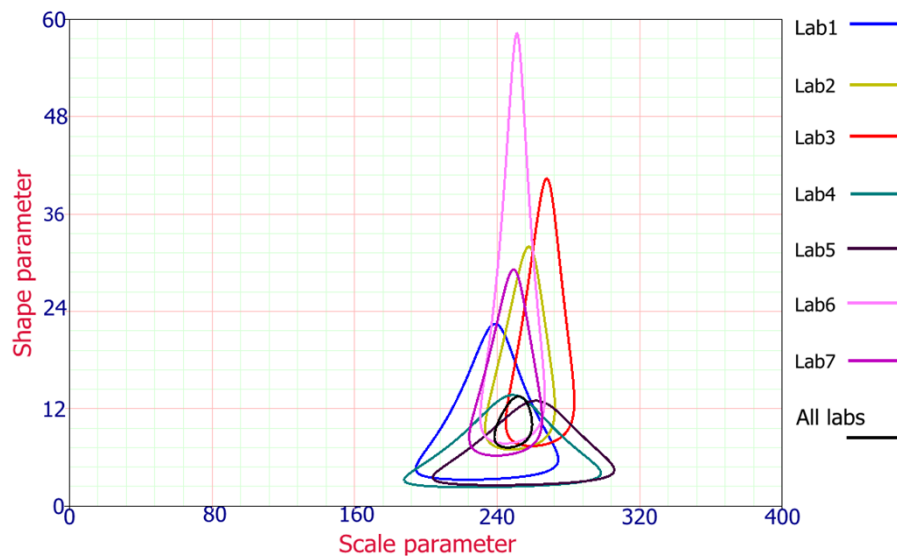


Figure 15: Weibull distribution based 95% confidence bounds for ultimate tensile strength.

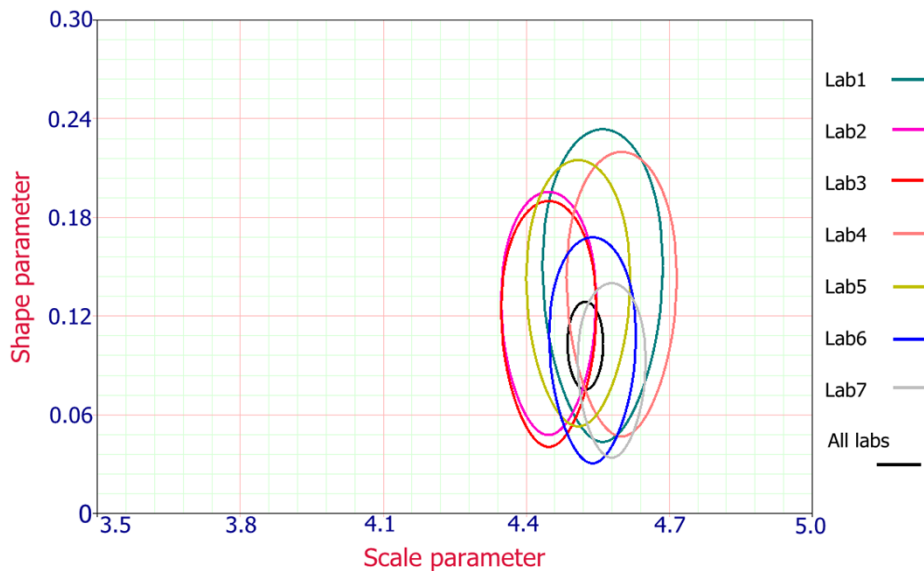


Figure 16: Lognormal distribution based 95% confidence bounds for proportional limit stress.

4.2 Precision and Bias Statements

When specimens of a presumably identical material are tested under presumably identical conditions within and between laboratories, the test data often have significant statistical variation. Apart from the random variation in the material itself, operators, test equipment and environmental factors also contribute to the variability in the test results. If the tests are conducted over a larger span of time then the variation in the results is usually greater. The differences in calibration of the equipment can contribute to variability in the test results. Thus, there are many factors which lead to variability in the results and these factors vary within a given laboratory and also between different laboratories. It is important to take into account the variability caused due to these factors before the test data can be used for any particular application. For instance, if two materials A and B are compared for tensile strength and the values obtained for material A are higher, then it may be not because material A is stronger than material B but it could be due to variability in the test conditions.

The closeness of a test result to the accepted reference value is generally termed as accuracy. The standard test methods report this accuracy in terms of precision and bias. The ASTM definition of precision is the closeness of agreement between independent test results on the same property of identical test material, expressed in terms of *repeatability* and *reproducibility*. Repeatability refers to the accuracy and random variability of the results obtained with the same method on identical test items in the same laboratory by the same operator using the same equipment within short intervals of time within a single laboratory. Reproducibility refers to the accuracy and random variability associated with successive measurements of the same property carried out by operators working in different laboratories, each obtaining single results on identical test material when applying the same method. Thus, precision of a test method provides an estimate of the variation the user of the test method can expect, which in turn reflects the utility of the standard test method. The ASTM definition of bias is the difference between the expectation of the test results and an accepted reference value

The precision statistics were calculated from the round robin data in accordance with ASTM E691-09 standard and are shown in Table 4. The precision statement for this study is stated below:

An interlaboratory test program gave the following precision statistics (Table 4) for the most commonly measured tensile properties of a CMC (SiC/SiC with HNLS fiber, CVI SiC matrix, PyC interphase) tube with nominal fiber volume fraction of 51%, an average bulk density of 2.71 g/cm³, and an average open porosity of 14%.

Table 4: Precision statistics calculated from the interlaboratory round robin data.

Mechanical Property	\bar{x}	s_x	s_r	s_R	r	R
UTS (MPa)	236.4623	13.2751	28.7144	29.7146	80.4	83.2
PLS (MPa)	91.9774	7.0779	8.4193	10.5288	23.6	29.5
Young's modulus (GPa)	201.9270	31.1474	30.5109	42.0486	85.4	117.7
Strain at failure (%)	0.5286	0.0608	0.0862	0.1003	0.24	0.28
Strain at PLS (%)	0.0566	0.0036	0.0063	0.0069	0.02	0.02

\bar{x} : mean of the laboratory means s_x : standard deviation of laboratory means s_r : repeatability standard deviation

s_R : reproducibility standard deviation

r: 95% repeatability limit (within laboratory) for 7 laboratories and 5-7 tests for each laboratory

R: 95% reproducibility limit (between laboratories) for 7 laboratories and 43 tests

No statement of bias can be made because no acceptable standard reference material exists.

5. DISCUSSION

5.1 Effect of Dimension Measurement Technique on Statistics

Since, the dimensional measurement of the specimens is an integral part of calculating the mechanical properties, accurate measurement of dimensions is very important. However, the roughness of the SiC/SiC composites used in this study surface makes it difficult to measure external dimensions accurately using tools such as calipers or micrometers. Therefore, the dimensions of the specimen used in this study were measured using radiography, as discussed in section 3.1. However, for the purpose of highlighting the influence of dimension measurement technique on the evaluated properties, a comparison was performed for a laboratory (Lab5) data. The data is for 7 specimens. In addition to radiography, the dimensions were also measured with a Vernier caliper. Some of the specimens, which failed in the cylindrical-to-conical transition region, were sectioned after the test to measure the dimensions. Since the failure strain of this material is very small (~0.5%) it is reasonable to assume that the dimension after the test is same as that before the test.

The outer diameter and wall-thickness were measured at three different locations along the gage length; at each location measurements were made at angles 0°, 60° and 120° as described in section 3.1 for radiography technique. The cross-sectional area was calculated using the mean outer diameter and wall thickness obtained from the nine measurements for each specimen. Table 5 shows the dimensions measured by the radiography and caliper. As can be noted from the table, the difference in the wall thickness measurement leads to significant difference in the cross-sectional area: area calculated using caliper is over 15% greater than the area measured using radiography. The properties evaluated using both the dimensions were compared. Table 6 shows the evaluated properties. The mean cross-sectional area of the specimens measured by the two methods differs by 18%. As can be noted from Table 6 the difference in UTS, PLS and Young's modulus based on the two dimensions is over 15% indicating a strong influence of the dimension measurement technique on the calculated properties statistics.

Table 5: Comparison of dimensions of SiC/SiC tubular specimens (7 specimen) measured using radiography and vernier caliper.

	Outer diameter (mm)		Wall thickness (mm)		Cross-sectional area (mm ²)	
	Mean	COV (%)	Mean	COV (%)	Mean	COV (%)
Radiography	9.51	0.50	0.78	3.94	21.41	3.61
Caliper	9.73	0.78	0.90	3.77	25.26	3.54
Difference in mean (%)	2.3		13.3		15.2	

Table 6: Comparison of properties evaluated using radiography and caliper based dimensions for laboratory Lab5.

	Cross-sectional area (mm ²)		Ultimate tensile strength (MPa)		Proportional limit stress (MPa)		Young's modulus (GPa)	
	Mean	S.D.	Mean	S.D.	Mean	S.D.	Mean	S.D.
Radiography based dimensions	21.41	0.77	233.2	45.3	91.2	9.0	202.4	19.6
Caliper based dimensions	25.26	0.89	198.0	40.5	77.2	6.4	171.3	13.7
Difference in mean (%)	-18.0		15.1		15.4		15.4	

The reason for difference in the measurement of cross-sectional area for the two methods is illustrated in Figure 17. The wall-thickness measured by the caliper is greater than that measured by the radiography. The dimensions measured by the radiography are based on the image analysis and the distance between the two surfaces can be directly measured by calculating the pixel and calibrating the pixels to real length. Thus, the limitations imposed by the surface roughness of the specimen are not applicable for the radiography technique. For the same reason the dimensions measured by micro-computed tomography are expected to be more accurate than that measured using mechanical instrument such as caliper or micrometer.

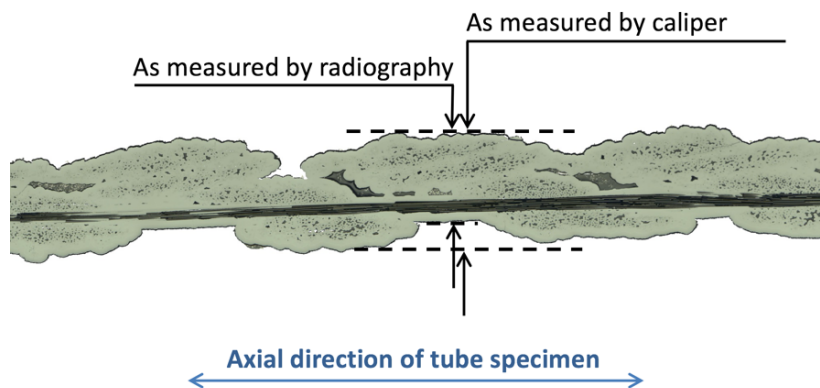


Figure 17: Measurements on a specimen wall; the surface roughness of the composite specimen leads to inaccurate measurement of the wall thickness by caliper, compared to radiography.

5.2 Method for Measuring Young's Modulus

It was noted that the method significantly influences the value of calculated Young's modulus. The stress-strain data from Lab3 was analyzed in two ways: (1) Lab3 calculated the Young's modulus considering data in 0.01 – 0.04% strain range 2) ORNL recalculated Young's modulus considering data in the 0.005 – 0.04% strain range. In the both the calculations, a line was linearly fit to the stress-strain data. The Young's modulus determined by ORNL was about 18% higher than that determined and reported by the Lab3. The significant difference in the value of the Young's moduli independently determined by both the laboratories highlights the importance of standardizing the procedure for calculating Young's modulus. A procedure below is proposed for calculating the Young's modulus and proportional limit stress.

Perhaps the main contribution to variation in the determined Young's modulus across different laboratories comes from the difference in the region of the stress-strain curve which is selected to determine the Young's modulus. Therefore, to have consistency in the procedure employed for calculating the modulus, the strain range should be defined instead of selecting it arbitrarily. For defining this strain range let's consider the following steps (see Figure 18): 1) first the slope of the stress-strain curve should be evaluated for the entire linear strain range 2) the slope of stress-strain curve is plotted against strain 3) the highest region of the curve, where the slope is maximum, is taken as the strain range for calculating the Young's modulus. The upper and lower limit of this range can be defined based on the allowed variability in the proportional limit stress that these limits will introduce. A linear fit is made to the data in this strain range. The slope of the linear fit is the Young's modulus of the specimen. From the lowest point of this range a line is extended down to the strain axis with its slope as the modulus. The intercept of this extended line with the strain axis is intercept A. The stress-strain curve is then shifted left by distance A. This shifting of the curve is performed to remove the 'toe' at the beginning of the curve which is usually associated with slack in the load train. The proportional limit stress is determined based on the shifted stress-strain curve using the appropriate offset which will vary from material to material.

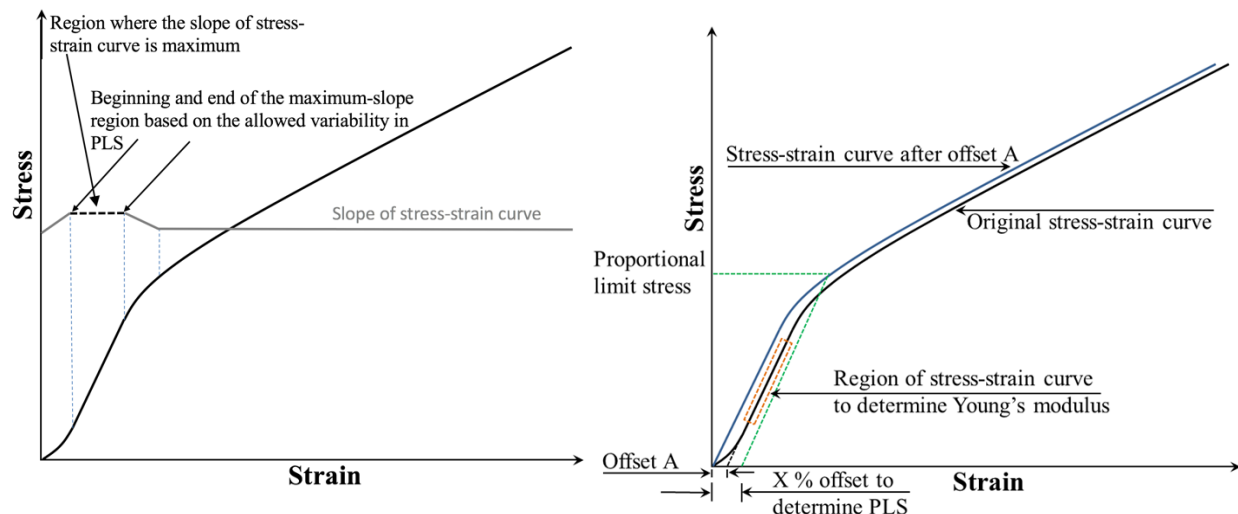


Figure 18: Proposed method to determine the Young's modulus and proportional limit stress.

5.3 Transition section failures vs Mid-Gage section failures

Test specimens failed in the mid-gage section as well as in the transition section as shown in Figure 19. Here the transition section refers to the section where the straight cylindrical gage region transitions

into the conical grip section of the specimen. Ideally the specimen should fail in the mid-region of the straight cylindrical section, but 33 of 43 specimens failed in the transition section. A comparison of the statistics was made to understand if the statistics of the properties for the specimens that failed in transition section are different from the statistics for specimens that failed in mid-gage section. Table 7 shows the comparison of the statistics. As can be noted from Table 7, the differences in the mean values are less than 8% for all the properties. The strain at PLS is same for both the failure types; the difference in PLS and strain at failure is less than 2%; the difference in UTS is less than 5% and for Young's modulus the difference is less than 8%. The same strain at PLS, and small differences in other properties indicate that the effect of failure locations had negligible effect on the mechanical properties.



Figure 19: Specimens with failure in transition section (leftmost specimen) and mid-gage section.

Table 7: Comparison of the material properties obtained from the specimens that failed in the mid-gage section and transition section.

	Test Count	Ultimate tensile strength (MPa)		Proportional limit stress (MPa)		Young's modulus (GPa)		Strain at failure (%)		Strain at PLS (%)	
		Mean	S.D.	Mean	S.D.	Mean	S.D.	Mean	S.D.	Mean	S.D.
Mid-gage section failures	10	229.6	21.9	91.3	7.8	191.2	41.4	0.52	0.08	0.057	0.004
Transition section failures	33	239.0	31.4	93.0	9.4	206.1	39.9	0.53	0.10	0.057	0.007
Difference in mean %		-4.1		-1.9		-7.8		-1.9		0	

5.4 Failure mode

A typical stress-strain curve obtained from the tests is shown in Figure 20. The stress-strain curve for composites essentially has three regions: 1) initial linear region which has highest slope, 2) the mid-region which is curved and the slope reduces continuously in this region and 3) the remaining region of the curve. When the specimen is initially loaded in tension the load is shared by the both the fibers and matrix. This loading range constitutes the first region of the stress-strain curve. The matrix, being weaker than the fibers, starts microcracking (at the strain of about 0.0005 for the specimens used in the present study). With increasing load, damage accumulates in the matrix, the cracks start propagating and run into the interphase which deflects the cracks around the fibers. Cracking of the interphase leads to debonding of fibers from

the matrix. This loading range where matrix damage is accumulating constitutes the second region of the stress-strain curve. Since the damaged matrix is not able to sustain the load, the entire load is transferred to the fibers. In this loading range, which constitutes the third part of the stress-strain curve, slope angle is smaller than that in the first region of the curve. Figure 21 shows the fiber pull-out in the tested specimen indicating a high toughness non-brittle failure mode with the typical composite failure.

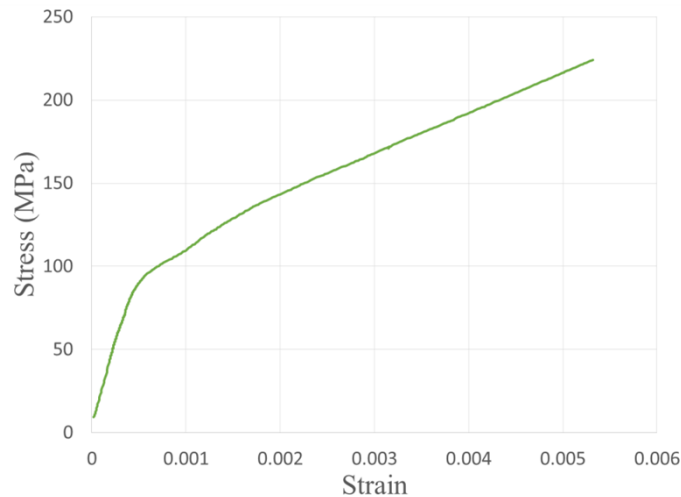


Figure 20: A typical tensile stress-strain curve obtained from the round robin tests.

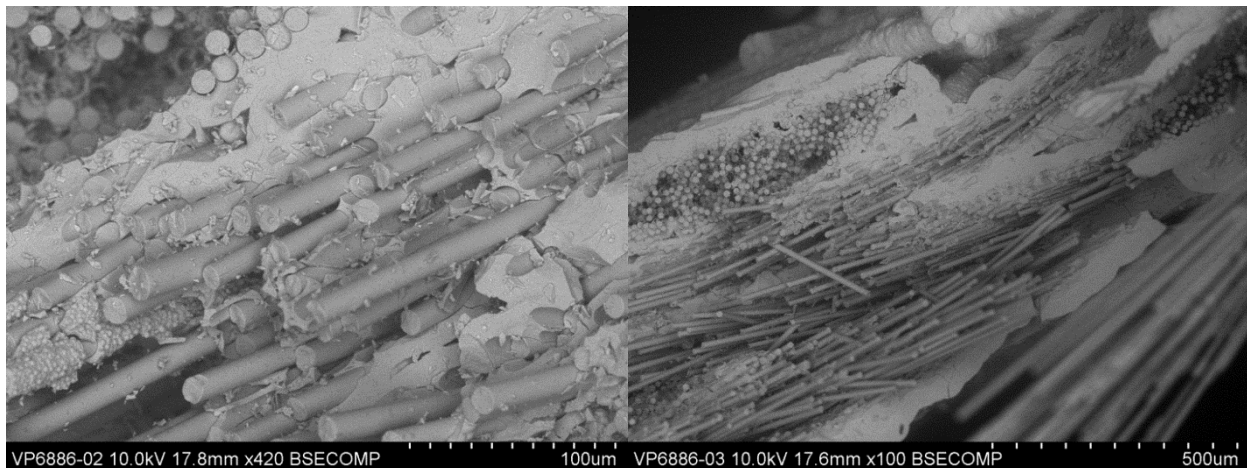


Figure 21: SEM image of the fractured cross-section surface of a tested SiC/SiC tubular specimen.

6. SUMMARY

A round robin testing program was carried out to determine the precision of the ASTM C1773 standard and expand the database of the mechanical properties of nuclear grade SiC/SiC composite material. The mechanical properties statistics for nuclear grade SiC/SiC composite tubular specimens were presented. In general, the data show reasonable consistency across the laboratories, indicating that the current C1773-13 ASTM standard is adequate for testing ceramic fiber reinforced ceramic matrix composite tubular specimens. The limited statistical variation in the mechanical properties demonstrate that the quality of the SiC/SiC material employed in these tests is appropriate for meeting the nuclear applications requirements regarding the mechanical properties. The ultimate tensile strength data seems to follow the 2-parameter

Weibull distribution with shape and scale parameters as 10.1 and 249.1 respectively. The proportional limit strength data fit best with the lognormal distribution, for the tested material.

It was found that the measured dimensions for tubular composite specimens vary with different measurement techniques - radiography versus mechanical method of measurement (micrometer, caliper). Therefore, the dimensional measurement technique can significantly influence the measurement of the cross-sectional area and then the calculated mechanical properties. Advanced techniques such as radiography and micro-computed tomography should be preferred over conventional mechanical methods. The work also brought forward the vagueness in the existing method for determining Young's modulus, which can lead to significant variation in the determined values across the laboratories. A method was proposed with the motivation of standardizing the procedure for modulus measurement.

ACKNOWLEDGEMENT

The authors would like to thank Charles Shane Hawkins, Don Erdman, Rick Lowden and Chris Stevens from ORNL for their technical support for the mechanical testing. Research sponsored by the Advanced Fuels Campaign of the Nuclear Technology R&D program, Office of Nuclear Energy, US Department of Energy, under contract DE-AC05-00OR22725 with UT-Battelle, LLC. The institutions participating in the inter-laboratory round robin testing campaign, besides Oak Ridge National Laboratory, are acknowledged: General Atomics, United Technology Research Center, Westinghouse – University of Virginia, NASA Glenn Research Center, Southern Research Institute, General Electric – Aviation.

7. REFERENCES

- [1] J. Carmack, F. Goldner, S. M. Bragg-Sitton, and L. L. Snead, "Overview of the US DOE accident tolerant fuel development program," in *Proc. 2013 LWR Fuel Performance Meeting/TopFuel 2013*, 2013, pp. 15-19.
- [2] S. J. Zinkle, K. A. Terrani, J. C. Gehin, L. J. Ott, and L. L. Snead, "Accident tolerant fuels for LWRs: A perspective," *Journal of Nuclear Materials*, vol. 448, pp. 374-379, 2014.
- [3] K. Yueh, D. Carpenter, and H. Feinroth, "Clad in clay," *Nuclear Engineering International*, vol. 55, pp. 14-16, 2010.
- [4] K. Yueh and K. A. Terrani, "Silicon carbide composite for light water reactor fuel assembly applications," *Journal of Nuclear Materials*, vol. 448, pp. 380-388, 2014.
- [5] K. E. Barrett, M. Teague, I. J. Van Rooyen, S. M. Bragg-Sitton, K. Ellis, C. Glass, *et al.*, "Engineering challenges of LWR advanced fuel cladding technology in preparation for in-reactor demonstrations," Oak Ridge National Laboratory (ORNL)2012.
- [6] S. Fazluddin, K. Smit, and J. Slabber, "The use of advanced materials in VHTR's," in *Second International Topical Meeting on High Temperature Reactor Technology*, 2004.
- [7] A. Kohyama, T. Hinoki, T. Mizuno, T. Kunugi, M. Sato, Y. Katoh, *et al.*, "R& D of Advanced material systems for reactor core component of gas cooled fast reactor," in *Proceedings of the International Congress on Advances in Nuclear Power Plants*, 2005, p. 19.
- [8] A. Raffray, R. Jones, G. Aiello, M. Billone, L. Giancarli, H. Golfier, *et al.*, "Design and material issues for high performance SiC f/SiC-based fusion power cores," *Fusion Engineering and Design*, vol. 55, pp. 55-95, 2001.
- [9] N. B. Morley, Y. Katoh, S. Malang, B. A. Pint, A. Raffray, S. Sharafat, *et al.*, "Recent research and development for the dual-coolant blanket concept in the US," *Fusion Engineering and Design*, vol. 83, pp. 920-927, 2008.
- [10] Y. Katoh and K. A. Terrani, "Systematic Technology Evaluation Program for SiC/SiC Composite-based Accident-Tolerant LWR Fuel Cladding and Core Structures: Revision 2015," Oak Ridge National Laboratory (ORNL)2015.
- [11] M. G. Jenkins, E. Lara-Curzio, S. T. Gonczy, and L. P. Zawada, "Multiple-Laboratory Round-Robin Study of the Flexural, Shear, and Tensile Behavior of a Two-Dimensionally Woven Nicalon™/Sylramic™ Ceramic Matrix Composite," in *Mechanical, Thermal and Environmental Testing and Performance of Ceramic Composites and Components*, ed: ASTM International, 2000.
- [12] Y. Katoh, K. Ozawa, C. Shih, T. Nozawa, R. J. Shinavski, A. Hasegawa, *et al.*, "Continuous SiC fiber, CVI SiC matrix composites for nuclear applications: Properties and irradiation effects," *Journal of Nuclear Materials*, vol. 448, pp. 448-476, 2014.
- [13] T. Nozawa, K. Ozawa, Y.-B. Choi, A. Kohyama, and H. Tanigawa, "Determination and prediction of axial/off-axial mechanical properties of SiC/SiC composites," *Fusion Engineering and Design*, vol. 87, pp. 803-807, 2012.
- [14] S. W. Tsai and E. M. Wu, "A general theory of strength for anisotropic materials," *Journal of composite materials*, vol. 5, pp. 58-80, 1971.
- [15] E. Rohmer, E. Martin, and C. Lorrette, "Mechanical properties of SiC/SiC braided tubes for fuel cladding," *Journal of Nuclear Materials*, vol. 453, pp. 16-21, 2014.
- [16] C. Deck, G. Jacobsen, J. Sheeder, O. Gutierrez, J. Zhang, J. Stone, *et al.*, "Characterization of SiC-SiC composites for accident tolerant fuel cladding," *Journal of Nuclear Materials*, vol. 466, pp. 667-681, 2015.
- [17] F. Bernachy-Barbe, L. Gélébart, M. Bornert, J. Crépin, and C. Sauder, "Anisotropic

- damage behavior of SiC/SiC composite tubes: Multiaxial testing and damage characterization," *Composites Part A: Applied Science and Manufacturing*, vol. 76, pp. 281-288, 2015.
- [18] T. Koyanagi, Y. Katoh, K. Ozawa, K. Shimoda, T. Hinoki, and L. L. Snead, "Neutron-irradiation creep of silicon carbide materials beyond the initial transient," *Journal of Nuclear Materials*, vol. 478, pp. 97-111, 2016.
- [19] H. M. Yun and J. A. DiCarlo, "Comparison of the tensile, creep, and rupture strength properties of stoichiometric SiC fibers," in *Proceedings of the 23rd annual conference on composites, materials and structures*, 1999, pp. 259-72.
- [20] A. Urano, J.-i. Sakamoto, M. Takeda, Y. Imai, H. Araki, and T. Noda, "Microstructure and Mechanical Properties of SiC Fiber" Hi-Nicalon Type S" Reinforced SiC Composites," in *22nd Annual Conference on Composites, Advanced Ceramics, Materials, and Structures-A: Ceramic Engineering and Science Proceedings, Volume 19*, 2009, p. 55.
- [21] M. Takeda, J. Sakamoto, A. Saeki, and H. Ichikawa, "Mechanical and structural analysis of silicon carbide fiber Hi-Hicalon type S," in *Ceramic Engineering and Science Proceedings*. vol. 17, No. 4, ed Westerville, OH: American Ceramic Society, 1996, pp. 35-42.
- [22] H. Ichikawa, "Polymer-Derived Ceramic Fibers," *Annual Review of Materials Research*, 2016.
- [23] R. J. Kerans, R. S. Hay, T. A. Parthasarathy, and M. K. Cinibulk, "Interface Design for Oxidation-Resistant Ceramic Composites," *Journal of the American Ceramic Society*, vol. 85, pp. 2599-2632, 2002.
- [24] R. Naslain, "Design, preparation and properties of non-oxide CMCs for application in engines and nuclear reactors: an overview," *Composites Science and Technology*, vol. 64, pp. 155-170, 2004.
- [25] T. Noda, H. Araki, H. Suzuki, and F. Abe, "Processing of carbon fiber/SiC composite for low activation," *Materials Transactions, JIM*, vol. 34, pp. 1122-1129, 1993.
- [26] A. Kohyama, "Present status of NITE-SiC/SiC for advanced nuclear energy systems," in *31st International Conference on Advanced Ceramics and Composites, Daytona Beach*, 2007.
- [27] T. Koyanagi, K. Ozawa, T. Hinoki, K. Shimoda, and Y. Katoh, "Effects of neutron irradiation on mechanical properties of silicon carbide composites fabricated by nano-infiltration and transient eutectic-phase process," *Journal of Nuclear Materials*, vol. 448, pp. 478-486, 2014.
- [28] Y. Katoh, T. Nozawa, C. Shih, K. Ozawa, T. Koyanagi, W. Porter, *et al.*, "High-dose neutron irradiation of Hi-Nicalon Type S silicon carbide composites. Part 2: Mechanical and physical properties," *Journal of Nuclear Materials*, vol. 462, pp. 450-457, 2015.
- [29] L. Alva, K. Shapovalov, G. M. Jacobsen, C. A. Back, and X. Huang, "Experimental study of thermo-mechanical behavior of SiC composite tubing under high temperature gradient using solid surrogate," *Journal of Nuclear Materials*, vol. 466, pp. 698-711, 2015.
- [30] C. Deck, H. Khalifa, B. Sammulu, T. Hilsabeck, and C. Back, "Fabrication of SiC-SiC composites for fuel cladding in advanced reactor designs," *Progress in Nuclear Energy*, vol. 57, pp. 38-45, 2012.
- [31] J. Zhang, H. Khalifa, C. Deck, J. Sheeder, and C. Back, "Thermal diffusivity measurement of curved samples using the flash method," *Ceramic Materials for Energy Applications V: Ceramic Engineering and Science Proceedings, Volume 36*, p. 43, 2015.

- [32] D. Kim, H.-G. Lee, J. Y. Park, and W.-J. Kim, "Fabrication and measurement of hoop strength of SiC triplex tube for nuclear fuel cladding applications," *Journal of Nuclear Materials*, vol. 458, pp. 29-36, 2015.

APPENDIX 1 - ILS PARTICIPATION AGREEMENT

PARTICIPATION AGREEMENT

ORNL and ASTM C28 INTERLABORATORY STUDY (ILS) ROUND ROBIN
ON AXIAL TUBE CMC TENSILE TESTING
June 2016 – July 2016

Our organization _____ located in _____ agrees to participate in the 2016 ASTM C28 ILS round robin on Axial Tube Tensile Testing of Ceramic Matrix Composites under the following terms and conditions:

1. We accept the set of SiC-SiC CMC tube test specimens and we will test them per the included project documents – ILS round robin ATT test plan and ASTM C1773. (*See the task list on the following page.*)
2. This testing will be done as a no-cost, in-kind participation in the ILS round robin project.
3. The CMC tube specimens will be used exclusively for the ILS round robin test. We will not do any other property testing or chemical/structural analysis on the CMC test specimens.
4. The CMC tube specimens are subject to U.S. federal export control requirements and will be protected and handled in accordance with applicable laws and regulations (ECCN: 1C007).
5. We will return all the fractured test specimens and the gripping system (fixtures, collets and swivel joints) after completion of testing to the project coordinator Gyanender Singh (Tel: (865) 574-5880, E-mail: singhgp@ornl.gov).

Signature

Date

Printed Name and Title

Please complete, sign, and return this agreement by e-mail or FAX before the start of testing to Gyanender Singh, ORNL, singhgp@ornl.gov Fax: (865) 241-3650.

APPENDIX 2 – GENERAL INSTRUCTIONS FOR CMC AXIAL TENSILE TUBE STRENGTH ILS STUDY

Objective

The objective of this ILS is to:

Determine the repeatability and reproducibility of the axial tensile tube (ATT) test method (ASTM C 1773) at ambient temperatures with one primary tube geometry for a SiC-SiC ceramic composite. The properties of interest are tensile ultimate strength and strain, proportional limit stress and strain, and elastic modulus in tension.

Materials

There is one (1) set of CMC ATT test specimens provided for the ILS study. Each set contains 8 test specimens.

The SiC-SiC ATT test specimens have been cut, finished, and measured at General Atomics and ORNL per the C1773 test standard. The specimens have been marked and logged with specimen identification numbers.

Test Specimens	
Composite	SiC-SiC composite tubes - Two-dimensional ($\pm 55^\circ$) triaxial braiding with two braid layers of Hi-Nicalon type S SiC fibers (monolayer PyC interface) with CVI SiC matrix. Produced by General Atomics Inc.
Specimen Geometry and Size	6" (150 mm) long tube with 8° tapered shoulders. Gage OD: 0.39" (10 mm), Gage ID: 0.34" (8.6 mm), Nominal Wall Thickness: 0.028" (0.7 mm), Gage length: 2.76" (70 mm)
Nominal Composite Mechanical Properties	Tensile Strength: 150-200 MPa , Strain at Failure: 0.5% , Prop. Limit (PL) Stress (0.01% offset): 60-90 MPa PL Strain: ~0.06 % Elastic Modulus: 150-200 GPa Failure Mode: semi-brittle, pseudo-ductile
Dimensional Tolerances	Per spec at General Atomics
Specimen Preparation	Fabrication OD finish of all specimens at General Atomics
Visual Inspection	At ORNL and at each test laboratory
Measurement	OD and ID Dimensions (at ORNL and each laboratory) Ultrasound for wall thickness at ORNL and calipers pre- and post-test
Conditioning	None

Test Equipment and Experimental Parameters	
Test Temperature/ Environment	Ambient temperature, no environmental chamber nor furnace required. Humidity Measurement
Test Machine	Tensile loading with tensile load cell (5 kip - 22 kN capacity with 1% accuracy)
Fixtures	Split copper collets, grip fixture and swivel joints (supplied by ORNL)
X-Head Rate	0.0015 – 0.003 inch/s; typically 30-60 seconds failure time (suggested rate: 0.0005 inch/s for load < 200lbf and 0.0025 inch/s for higher load)
Extension and Strain Measurement	Strain measurement is required, either by clip-on extensometer/s (1" gage recommended) or by two or more strain gages.
Alignment and Bending Stress Check	Strain gaged alignment specimen provided by ORNL. Testing laboratories will check alignment in their systems.
Specimen Dimensions Measurement	Precision Calipers/Micrometers pre and post test. Ultrasound for wall thickness at ORNL
Measured and recorded test data	Applied force and extension/strain as a function of time/X-head movement.
Data Collection	Digital (force and extension/strain vs. time, and max force) Suggested collection rate – 40 points per second
Calculated data	Ultimate tensile strength, Ultimate tensile strain, Elastic modulus Proportional limit (PL) stress and PL strain (0.01% offset)
Fracture Analysis	Will be done at ORNL

The ILS test package contains the following items

1. Introduction letter
2. Participation agreement (Appendix 1) to use the specimens only for the axial tensile strength testing and return all the test specimens, alignment specimen and the gripping system (fixtures, collets and swivel joints) after the test.
3. Test instructions (Appendix 2) and a procedure checklist (Appendix 3).
4. A copy of the ASTM C1773 ATT test method, printed (Appendix 4).
5. One test specimen set with 8 ATT test specimens in each set, ready for testing.
6. An alignment specimen with applied resistance strain gages.
7. The two collet grip fixtures (top and bottom) for the ATT tests.
8. Copper split collets for the test specimens (8 sets of 4 half-split collets (2 top & 2 bottom)).
9. Two swivel joints.
10. The following items will be sent through email:
 - a) Data report in a MS- EXCEL™ spreadsheet format (ATTDataSheet.XLS),
 - b) Dimensions of the test specimens in a MS- EXCEL™ spreadsheet and
 - c) Pdf version of the ASTM C1773 ATT test method.
11. A printed copy of the MS- EXCEL™ data spread sheet format for your review. (Appendix 5)

Specific Tasks for the ILS ATT Test Laboratories

The ATT testing of the SiC-SiC tube test specimens will be done by six laboratories according to the ASTM C1773 test standard with their in-house testing test equipment, using the supplied grip fixtures, copper split collets and swivel joints.

The success and value of the ILS effort depends on three factors:

1. All of the CMC ceramic test specimens in each test set are uniform in physical and mechanical properties.
2. All of the participating laboratories prepare their equipment, measure the specimens, and perform the ATT tests according to the ASTM C1773 test standard (Appendix 4) and the procedure checklist (Appendix 3).
3. The participating laboratories complete the testing in a timely manner (no later than one month after receiving the specimens and fixtures unless agreed otherwise) and promptly return the Excel spread sheet file with all the formatted test data and fractured specimens to the test coordinator.

The specific tasks for the tensile testing laboratories are listed below. These tasks request information beyond the minimum requirements of ASTM C1773 to evaluate the robustness of the standard test method.

APPENDIX 3 – AXIAL TUBE TENSILE TESTING CHECKLIST

Return this completed check list with your test data for each test specimen set.

The tasks in the checklist request information beyond the requirements of the draft test standard to evaluate the robustness of the standard test method.

Technical Contact for ATT Testing:

Gyanender Singh
 Oak Ridge National Laboratory
 Tel: (865) 574-5880 E-mail: singhgp@ornl.gov

Laboratory Name		
Contact & Phone		
E-Mail Address		
Test Date		
ORNL SiC-SiC 05-16	Spec ID #	

The schedule for completing the testing and returning the test pieces to the ILS coordinator Gyanender Singh: no later than one month after receiving the specimens and fixtures unless agreed otherwise.

**There are six sections to
 this checklist:**

- 1 Initial Test Specimen Check and Planning**
- 2 Test Specimen Preparation**
- 3 Equipment Check and Set-up**
- 4 Tensile Testing (Ambient Temperature)**
- 5 Calculation, Data Recording & Review**
- 6 Return Data and Test specimens**

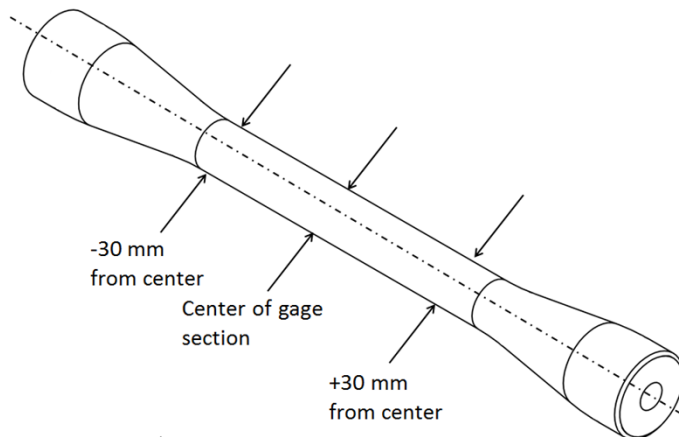
INITIAL TEST SPECIMEN CHECK & TEST PLANNING

<u>Step</u>	<u>Check Box</u>	<u>ACTION</u>	Reference to ASTM C1773
1	<input type="checkbox"/>	Count the number of test specimens against the shipping documents-eight (8) test specimens in the test set). Check each specimen for breaks, surface cracks, or warping. (Call the test coordinator, if the test specimen sets are incomplete or test specimens are broken, cracked, or damaged)	NA
2	<input type="checkbox"/>	Check the legibility of the specimen ID numbers on the test specimen packages.	NA

- | | | | |
|---|--------------------------|--|-------------------|
| 3 | <input type="checkbox"/> | Until ready to do the testing, the specimens should be stored in their original packaging in a controlled environment or desiccator to prevent handling damage and minimize temperature and humidity extremes. | Sec. 9.10 |
| 4 | <input type="checkbox"/> | Review the ASTM C1773 standard and these ILS instructions. | Test Instructions |
| 5 | <input type="checkbox"/> | Review the Excel data report spread sheet for format and content. | Test Instructions |
| 6 | <input type="checkbox"/> | Determine how the grip fixtures will fit into your test system load train, maintaining alignment and force application. | Test Instructions |

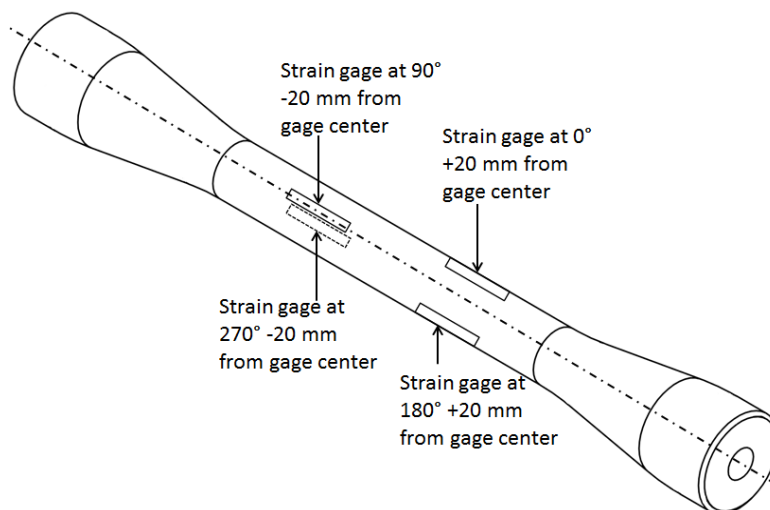
TEST SPECIMEN PREPARATION and MEASUREMENT

<u>Step</u>	<u>Check Box</u>	<u>ACTION</u>	<u>Reference to ASTM C1773</u>
1.	<input type="checkbox"/>	Open the packaging of the test specimens and check the test specimens and copper split collets for damage.	NA Sec 10.4.1
2.	<input type="checkbox"/>	Check the accuracy and calibration of your flat anvil micrometer and your knife edge calipers. <i>Use the micrometer for pre-test OD measurements.</i> <i>Use the calipers for post-test OD and wall thickness measurements.</i>	Sec. 7.3.7 Sec. 7.3.4
3.	<input type="checkbox"/>	Note and record the ID number for each test specimen.	Sec 10.3
4.	<input type="checkbox"/>	Measure and record outer diameter (d_o) of each test specimen at 9 points (3 points around the circumference at three locations (center, center - 30 mm, center + 30 mm) along the gage section length, with total 9 measurements) Measure to an accuracy of 0.01 mm.	



Measure and record the overall length of the test specimen and the length of the gage section (2 measurements). Measure to an accuracy of 1 mm.

5. If resistance strain gages (12 mm length suggested) are used, install the strain gages per the test standard and record the locations. Sec 7.3.2
Sec 10.3.3
 (**Minimum** of 2 strain gages -- at the center of the gage section, 180° apart.
Preferred – 4 strain gages -- 2 gages 20 mm down from gage center at 0° and 180° and 2 gages 20 mm up from gage center at 90° and 270°)



ATT TESTING

<u>Step</u>	<u>Check Box</u>	<u>ACTION</u>
-------------	------------------	---------------

Reference to ASTM
C1773

- | | | |
|----|--------------------------|---|
| 1. | <input type="checkbox"/> | Check the specimen ID numbers |
| 2. | <input type="checkbox"/> | Measure and record the ambient temperature and humidity at the beginning of the test session. |
| 3. | <input type="checkbox"/> | Position and center the test specimen with the copper split collets in the split collet grip fixture.

Mark the test specimen for orientation. |
| 4. | <input type="checkbox"/> | Strain Measurement:
Mount, connect, and check the extensometer gage on the test specimen.
OR
Connect and balance the strain gages, if they are used. |
| 5. | <input type="checkbox"/> | Activate and adjust the testing machine for initial cross-head position, zero load, displacement test mode, and cross head speed. |

Sec 10.11.1

Sec 10.7

Sec 10.6

Sec 10.9
Sec 10.10
and 10.11.26. Activate and check the data acquisition system.7. Preload the specimen with approximately 25-40 Newton to maintain specimen alignment.

Sec 10.11.2

8. Start the test by activating the cross-head movement and the data recorder.

Sec 10.11.3

 Record and store the force-strain data for each test.9. Apply force until the test specimen fractures or there is a drop of 50% from the maximum observed force

Sec 10.11.4

10. Measure and record the peak/failure force (Newton) and the failure strain (%) against the specimen ID #.

Sec 10.11.4

 Stop the data acquisition

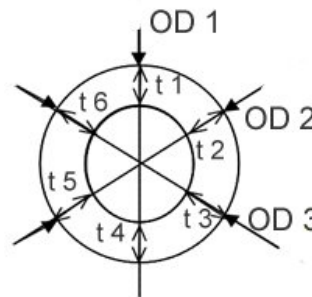
Sec.10.11.5

 Remove the broken specimen segments from the grip fixture.
Return the cross-head to the zero position.11. Note and record if the test is invalid or censored because of failure in the grip sections or outside the gage section.

Sec.10.12.1

12. With the calipers measure and record the OD and wall thickness on each specimen at three spans around the circumference close to the fracture point (3 OD measurements and 6 wall thickness measurements).

Sec. 10.13.1

13. Note and record where the fracture location is with respect to the center of the gage section (e.g., 10 mm up or down from the gage center)

Calculation, Data Recording and Data Review

<u>Step</u>	<u>Check Box</u>	<u>Action</u>	<u>Reference to ASTM C1773</u>
	<input type="checkbox"/>	Using the fracture force (N) and the original cross section area (mm ²) (based on average OD and wall thickness measurements), calculate the axial fracture strength (MPa) (This is done automatically in the EXCEL data sheet).	Sec. 11.4
	<input type="checkbox"/>	Using the elastic section of the stress-strain curve, calculate and record the tensile elastic modulus (GPa).	Sec. 11.5
	<input type="checkbox"/>	Using the 0.01% offset method against the elastic section of the stress-strain curve, calculate and record the proportional limit stress (MPa) (0.01% offset) and PL strain (%).	Sec. 11.7
	<input type="checkbox"/>	Record the test data (experimental parameters, specimen data, and test results) in the Excel spread sheet. (File: ATTDDataSheet.xls).	Sec. 12
	<input type="checkbox"/>	Review the report test data (test parameters, test specimen data, and test results- Appendix 5) and ensure that data are complete and accurate with no typographical errors	Sec. 12
	<input type="checkbox"/>	Transfer the force-extension/strain data for each test to the Excel spread sheets, identified by test specimen ID.	Test Instr.
	<input type="checkbox"/>	Save the completed Excel data spread sheet (File: ATTDDataSheet.xls).	Test Instr.

RETURN DATA AND TEST SPECIMENS

- Send the completed Excel data spreadsheet file along with the force-displacement data to Gyanender Singh by e-mail. (singhgp@ornl.gov) Test Instr.
- Prepare the test specimen package for shipping with the following: Test Instr.
The package with the broken test specimens.
Alignment specimen
A hardcopy of the completed checklist for the test specimen set.
- Prepare the gripping system package for shipping with the following:
Gripping system (fixtures, collets and swivel joints)
- Securely send the packages to:
Gyanender Singh
Oak Ridge National Laboratory || One Bethel Valley Road MS-6136
A-155, Building 4500S || Oak Ridge, TN 37831-6136
(865) 574-5880

The schedule for completing the testing and returning the test pieces to the ILS coordinator Gyanender Singh: within one month of receiving the test specimens and fixtures unless agreed otherwise.

APPENDIX 4 – INVITATION LETTER FOR THE INTERLABORATORY PARTICIPANTS

ILS -- Axial Tensile Strength of Ceramic Matrix Composite Tubes

ASTM C-28 ADVANCED CERAMICS COMMITTEE

Date

Name of laboratory contact
Organization name
Street Address
City, State PIN

Dear Potential participant name,

We are ready to begin our interlaboratory study (ILS) on the uniaxial tensile strength of ceramic matrix composite tubes, using the new ASTM C1773 Standard Test Method (Monotonic Axial Tensile Behavior of Continuous Fiber-Reinforced Advanced Ceramic Tubular Test Specimens at Ambient Temperature). The objective of this first ILS is to:

Determine the repeatability and reproducibility of the axial tensile tube (ATT) test method (ASTM C 1773) at ambient temperatures for a SiC-SiC ceramic composite with one primary tube geometry. The properties of interest are ultimate tensile strength and strain, proportional limit (0.01% offset) stress and strain, and elastic modulus in tension.

We have laid out a detailed experimental plan for the ILS, using a SiC-SiC composite tube with a defined geometry (6" long tube with 8° tapered shoulders, gage OD = 0.39", gage ID = 0.34", nominal gage length = 2.76"). The CMC tube test specimens will be tested at ambient temperature. Each test set will have 8 test specimens for each participating laboratory. (The full test plan and instructions are laid out in Appendix 2.)

Test specimen sets are being sent to you and 4 other laboratories for testing. This test package contains the following items:

1. Introduction letter
2. Participation agreement (Appendix 1) to use the specimens only for the axial tensile strength testing and return all the test specimens after the test.
3. Test instructions (Appendix 2) and a procedure checklist (Appendix 3).
4. A copy of the ASTM C1773 ATT test method, printed (Appendix 4).
5. One test specimen set with 8 ATT test specimens in each set, ready for testing.
6. An alignment specimen with applied resistance strain gages.
7. The two collet grip fixtures (top and bottom) for the ATT tests.
8. Copper split collets for the test specimens. (8 sets of 4 half-split collets (2 top & 2 bottom))
9. Two swivel joints.
10. The following items will be sent through email:
 - a) Data report in a MS- EXCEL™ spreadsheet format (ATTDataSheet.XLS),
 - b) Dimensions of the test specimens in a MS- EXCEL™ spreadsheet and
 - c) Pdf version of the ASTM C1773 ATT test method.
11. A printed copy of the MS- EXCEL™ data spread sheet format for your review. (Appendix 5)

With these test specimens, grip fixtures and swivel joints, collets, alignment specimen, and instructions, you have the materials and information needed to complete your portion of the ILS. The detailed ILS testing tasks are listed in Appendix 1, page 3 and in the ILS check list (Appendix 3)

The success and value of the ILS effort depends on three factors:

1. All of the CMC tube test specimens in each test set are uniform in physical and mechanical properties.
2. All of the participating laboratories prepare their equipment, measure the specimens, and perform the ATT tests according to the ASTM C1773 test standard (Appendix 4) and the test procedure checklist (Appendix 3).
3. The participating laboratories complete the testing in a timely manner and promptly return all the formatted test data, fractured test specimens and the gripping system (fixtures, collets and swivel joints) to the test coordinator.

For scheduling purposes, we would like the testing and data reporting to be completed within one month after you receive the test specimens and fixtures unless agreed otherwise.

If you have technical (samples or testing procedures) or administrative (data and reporting requirements, shipping/packaging) questions about this package and the test specimens, please contact:

Gyanender Singh/Yutai Katoh Oak Ridge National Laboratory Tel: (865) 574-5880 E-mail: singhgp@ornl.gov	Stephen T. Gonczy Gateway Materials Technology Inc. Tel: (847) 870-1621 E-Mail: gatewaymt@aol.com
---	--

Your participation in the ILS is much appreciated. We look forward to your contribution of time and effort to this technical project which supports aerospace and nuclear ceramic composites technology and the development of ASTM advanced ceramics standards.

Gyanender Singh/Yutai Katoh
Materials Science and Technology Division
Oak Ridge National Laboratory
Oak Ridge, TN 37831

Stephen Gonczy
Gateway Materials Technology
221 S. Emerson
Mount Prospect, IL 60056

APPENDIX 5 – TASK LIST FOR THE AXIAL TUBE TENSILE (ATT) TEST ILS STUDY

TASK LIST FOR THE AXIAL TUBE TENSILE (ATT) TEST ILS STUDY	
PACKAGE RECEIPT AND SPECIMEN CHECK	
1.	Check the test package for completeness -- the ILS instructions, the procedure checklist (Appendix 3), the ASTM C1773 standard (Appendix 4), and the included the 8 test specimens, grip fixtures, 8 collets sets, swivel joints, the alignment specimen, the test data report EXCEL file, and the specimen dimension Excel File.
2.	Review the test plan and procedures described in this letter and appendix. Review, sign, and return (e-mail or fax) the participation agreement (Appendix 2) to Gyanender Singh (singhgp@ornl.gov , Fax (865) 241-3650).
3.	Check the count and condition of the SiC-SiC specimens in the test set and store them in their original packaging in a desiccator until testing.
4.	Check the alignment specimen, the two grip fixtures and swivel joints, and the 8 sets of copper split collets for count and condition. Check how the grip fixtures will be fitted into your test system, accounting for proper alignment.
Specimen Tensile Testing	
5.	Review the ILS instructions, the procedures checklist (Appendix 3), and the ASTM C1773 test standard (Appendix 4).
6.	Set up and check the testing equipment for specimen insertion and alignment, force measurement, displacement control, and strain measurement, per the attached checklist (Appendix 3) and the ASTM C1773 test standard (Appendix 4)
7.	Complete 8 ATT tests per the attached checklist (Appendix 3) and the ASTM C1773 standard (Appendix 4). Use and complete the checklist to ensure proper testing.
8.	Measure and record the OD and wall thickness of each specimen at three points close to the fracture site.
9.	Record (in the MS-EXCEL file) and review the specimen data, experimental data, test data, and force-extension/strain data for completeness and accuracy. Send the completed data EXCEL spread sheet file by e-mail to Gyanender Singh (singhgp@ornl.gov)
10.	Collect, pack and send the fractured test specimens and completed checklists to Gyanender Singh at the address given below. Gyanender Singh Oak Ridge National Laboratory One Bethel Valley Road MS-6136 A-155, Building 4500S Oak Ridge, TN 37831-6136 (865) 574-5880

APPENDIX 6 – AXIAL TENSILE TEST STRESS-STRAIN CURVES FOR THE SiC/SiC SPECIMENS

Stress-strain curves for specimens 9, 10, 11, 12 and 13.

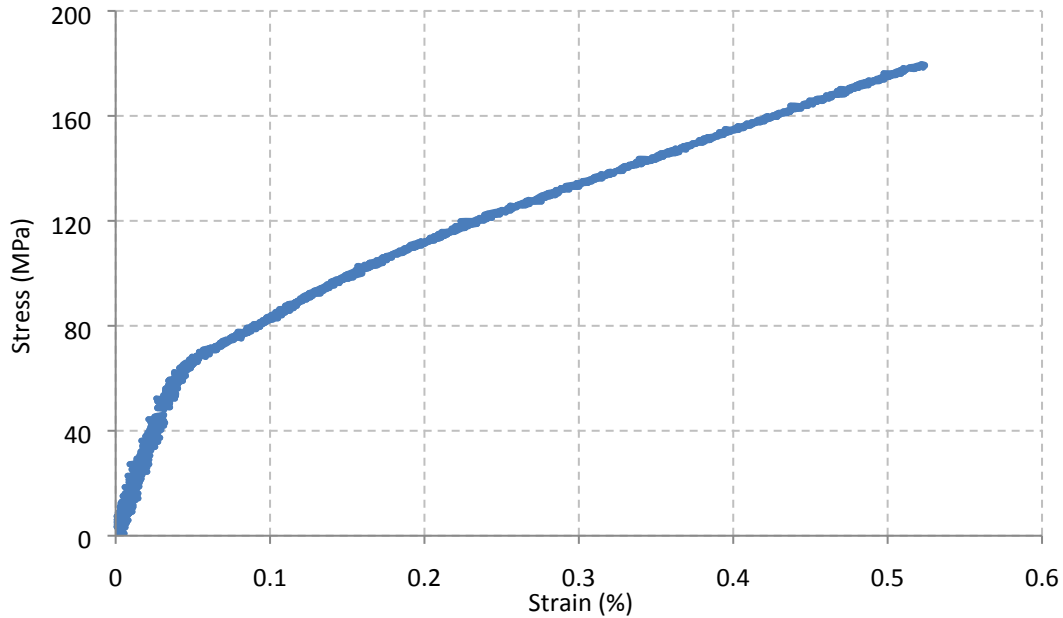


Figure 22: Stress-strain curve for specimen-9.

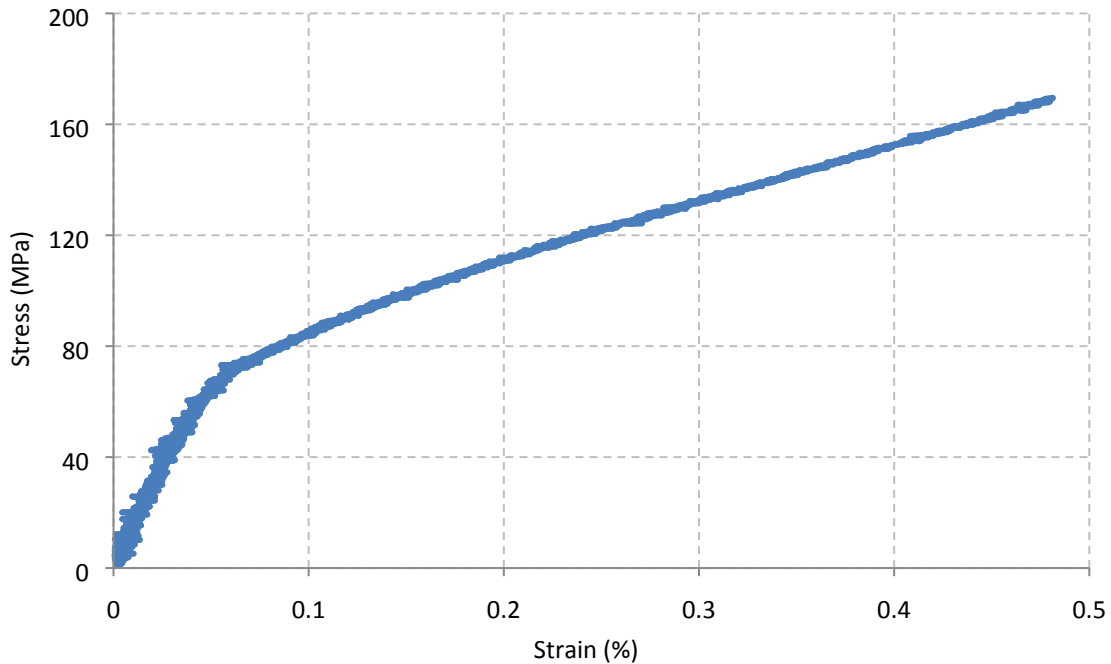


Figure 23: Stress-strain curve for specimen-10.

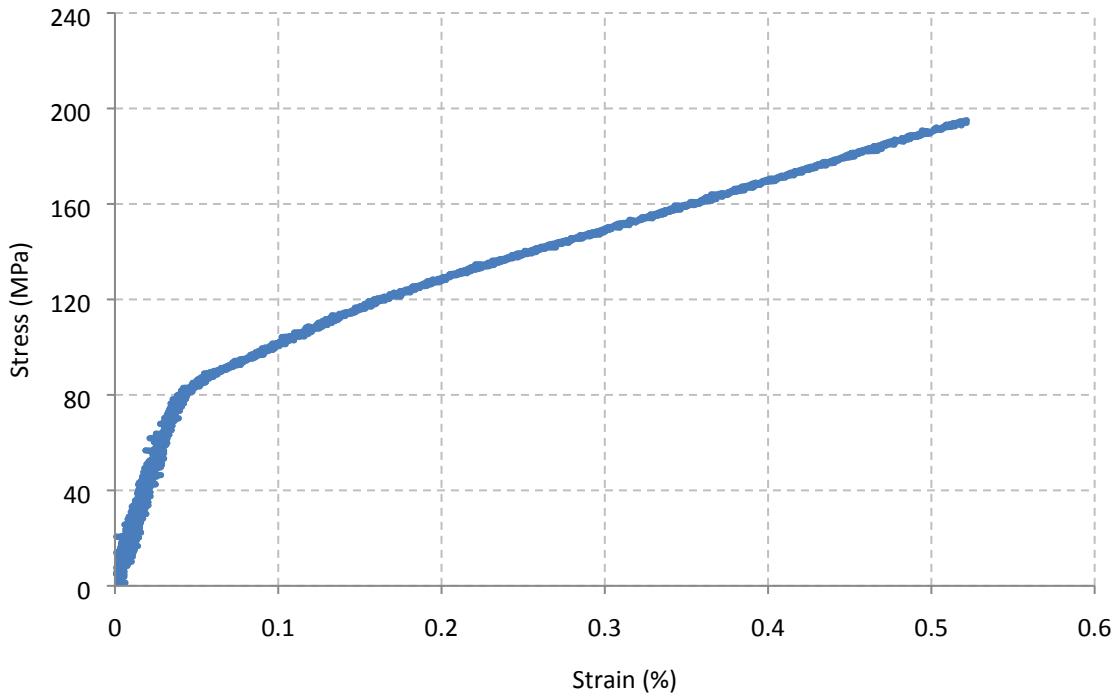


Figure 24: Stress-strain curve for specimen-11.

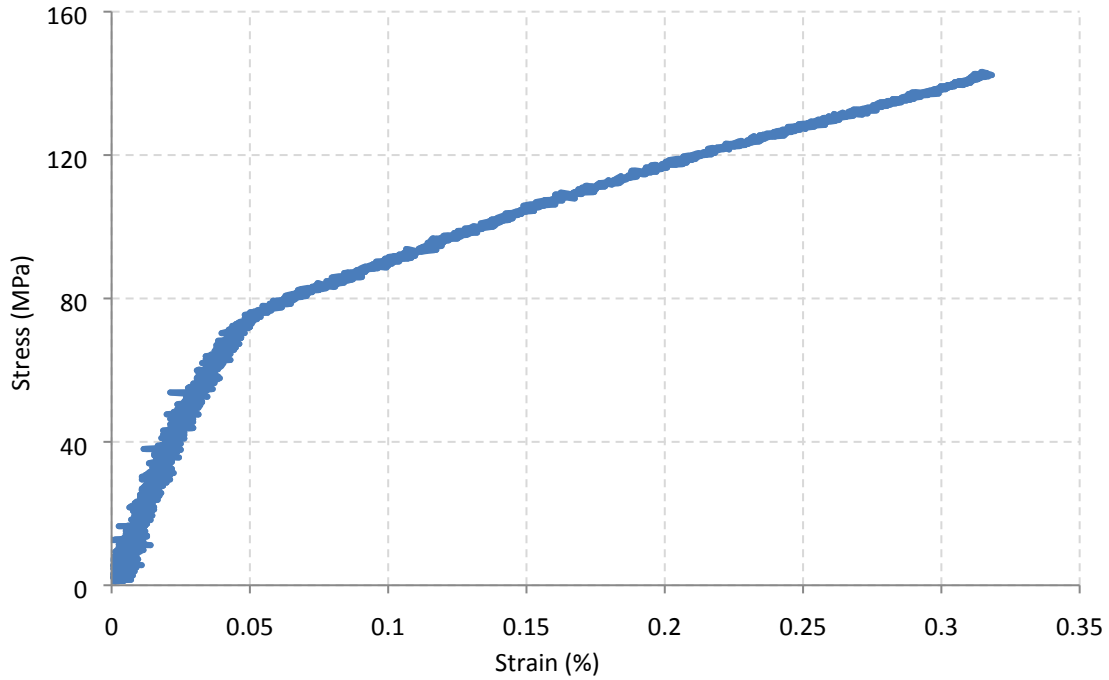


Figure 25: Stress-strain curve for specimen-12.

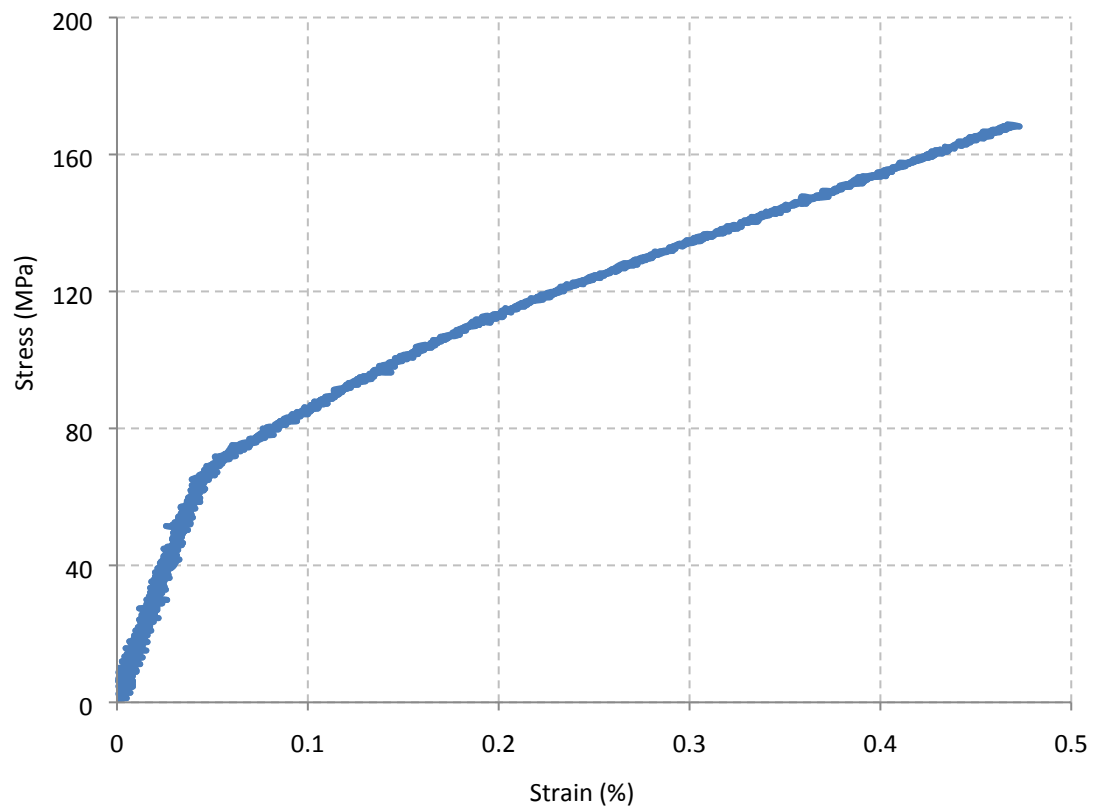


Figure 26: Stress-strain curve for specimen-13.